/
Article / Book Information

( )	HIF TOP3
Title(English)	Evaluation of the efficacy of HIF-targeting prodrug TOP3 in combination with chemotherapeutic drugs for pancreatic cancer treatment
( )	HoangThiHongNgoc
Author(English)	Thi Hong Ngoc Hoang
( )	: , : , : 10329 , :2016 9 20 , : , : , , , ,
Citation(English)	Degree:, Conferring organization: Tokyo Institute of Technology, Report number: 10329 , Conferred date:2016/9/20, Degree Type:Course doctor, Examiner:,,,,
( )	
Type(English)	Doctoral Thesis

Tokyo Institute of Technology

Graduate School of Bioscience and Biotechnology

Department of Biomolecular Engineering

Kondoh Laboratory

Evaluation of the efficacy of HIF-targeting prodrug TOP3 in combination with chemotherapeutic drugs for pancreatic cancer treatment

Hoang ThiHongNgoc

Advisor: Prof. Shinae Kondoh

Vice-advisor: Prof. Yoh-ichi Tagawa

-2016-

Table of Contents

Abbreviations

5-FU: 5-Fluorouracil

ANGPT: Angiopoietin

BCA: Bicinchoninic acid

bHLH: Basis helix-loop-helix

BLI: Bioluminescent imaging

BSA: Body surface area

CBB: Coomassie brilliant blue

CBP/p300: Cyclic AMP responsive element binding protein

CD: Cytidine deaminase

CDHP: 5-chloro-2, 4-dihydroxypyridine

CDP: Cytidine diphosphate

CMV: Cytomegalovirus

dCDP: Deoxycytidine diphosphate

dCK: Deoxycytidine kinase

DCTD: Deoxycytidine monophosphate deaminase

DFcCTP: Gemcitabine triphosphate

dFdC: 2',2'-Difluoro-2'-Deoxycytidine

dFdCDP: Gemcitabine diphosphate

dFdCMP: Gemcitabine monophosphate

dFdUMP: Difluoro-deoxyuridine monophosphate

DHFU: Dihydrofluorouracil

DMEM: Dulbecco's modified eagle medium

dUMP: Deoxyuridine monophosphate

dTMP: Deoxyuridine triphosphate

EDTA: Ethylenediaminetetraacetic acid

EGFR: Epidermal growth factor receptor

EPO: Erythropoietin

ERK: Extracellular-signal-regulated kinase

FBS: Fetal bovine serum

FdTDP: Fluorodeoxyuridine triphosphate

FdUDP: Fluorodeoxyuridine diphosphate

FLuc: Firefly luciferase

FOXO: Forkhead box O4

FUDP: Fluorouridine diphosphate

FUMP: Fluorouridine monophosphate

FUTP: Fluorouridine triphosphate

G6P: Glucose-6-phosphate

G6PD: Glucose-6-phosphate dehydrogenase

PEP: Phosphoenolpyruvic acid

GF: Growth factor

GI: Gastrointestinal

GLUT: Glucose transporter

GSK3: Glycogen synthase kinase 3

GST: Glutathione S-transferase

HIF: Hypoxia-inducible factor

HK: Hexokinase

H_2O_2: Hydrogen peroxide

HRE: Hypoxic responsive element

HSPG: Heparin sulphate proteoglycans

IC50: Half maximal inhibitory concentration

IGF: Insulin-like growth factor

IGFR: Insulin-like growth factor receptor

IPTG: Isopropyl β-D-1-thiogalactopyranoside

i.p.: intraperitoneal injection

IVIS: *In vivo* imaging system

LDH: Lactate dehydrogenase

MAPK: Mitogen-activated protein kinase

MDR-1: Multidrug resistance 1

mTOR: Mammalian target of Rapamicin

MTS: Membrane translocating sequences

NDK: Nucleoside diphosphate kinase

NIRF: Near-infrared fluorescent

OD: Optical density

ODD: Oxygen-dependent degradation domain

Oxo: Potassium oxonate

PAS: Per-Arnt-Sim

PDGFB: Platelet-derived growth factor B

PDH: Pyruvate dehydrogenase

PDK1: Pyruvate dehydrogenase kinase 1

PEP: Phosphoenolpyruvic acid

PGF: Placental growth factor

PHD: Prolyl hydroxylase

PI3K: Phosphatidylinositol 3-kinase

PKM2: Pyruvate kinase M2

PLB: Passive lysis buffer

p.o.: per os (oral administration)

POH: PTD-ODD-HaloTag

RACK: Receptor of activated protein C kinase

RLuc: Renilla luciferase

RNR: Ribonucleotide reductase

ROS: Reactive oxygen species

RPMI: Roswell park memorial institute

SDS-PAGE: Sodium dodecyl sulfate polyacrylamide gel electrophoresis

TAD: Transcriptional activation domain

TAT: Transactivator of transcription

TBST: Tris-buffered saline and 0.05% Tween 20

TCA: Tricarboxylic acid

TGF-α: Transforming growth factor-α

TOP3: TAT-ODD-Procaspase-3

TS: Thymidylate synthase

VEGF: Vascular endothelial cell growth factor

VHL: Von Hippel-Lindau

WST-1: Water soluble tetrazolium salt

Chapter 1

General introduction

1.   Intratumoral hypoxia

Intratumoral hypoxia, one of the refractory characteristics of solid tumors, develops as a result of an imbalance between the supply and consumption of oxygen when cancer cells outgrow [1]. The hypoxic region with limited level of oxygen and nutrition is located between normoxic and necrotic regions, and about 100 μm away from blood vessels. Hypoxia can influence tumor cells in one of two ways, either by acting as a stressor that impairs growth or causes cell death (deceleration of proliferation, apoptosis, or necrosis) or by serving as a factor that ultimately results in malignant progression and increased resistance to radiation therapy and other cancer treatments [2-4]. Particularly, low oxygen levels in hypoxic tumors decrease radiosensitivity since O_2 acts as a source of radiation-induced radicals that cause severe damage to cellular macromolecules, especially the DNA. [5]. On the other hand, the chemotherapeutic resistance can be a direct result of poor delivery of drugs or the indirect result of alterations in the proteome/genome in the cells responding to hypoxia [6]. (**Figure 1.1**)
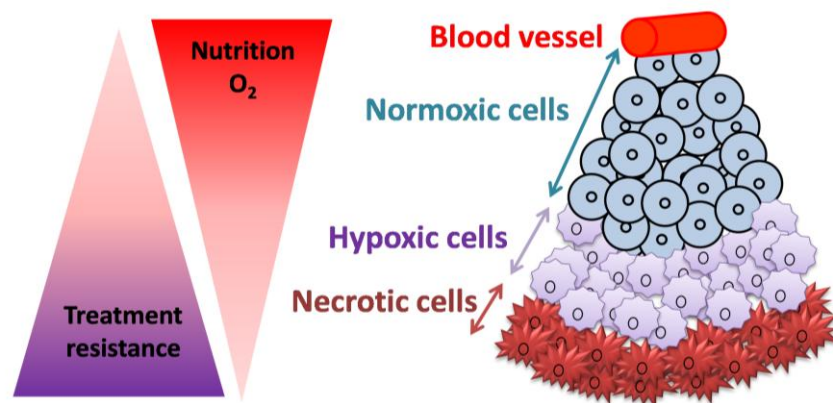

Figure 1.1. Location and characteristics of intratumoral hypoxia. Tumor hypoxia arises in regions with impaired oxygen delivery.

2.   Hypoxia-inducible factor-1 (HIF-1)

2.1.   HIFs protein family

Hypoxia-inducible factors (HIFs) are transcriptional activators that function as master regulators of cellular and systemic oxygen homeostasis and play critical roles in tumor hypoxia. There are three paralogues of HIF: HIF-1, HIF-2, HIF-3. HIF-1 is found in all tissues whereas the presence of HIF-2 and HIF-3 is limited to specific types of tissues.

Therefore, HIF-1 is extensively researched as a potential protein to understand cell behaviours under hypoxic conditions as well as hypoxic related diseases [7, 8].

Human HIF-1 is a heterodimer consisting of HIF-1α and HIF-1β subunits. HIF-1β (also known as aryl hydrocarbon nuclear translocator) is constitutively expressed in cells irrespective of oxygen presence. HIF-1α, on the other hand, has the synthetic mechanism independent of oxygen but the stability and transcriptional activity heavily depend on the oxygen level [9]. HIF-1α subunit has 826 amino acids in total. It contains the basic helix-loop-helix (bHLH) domain at the N-terminal end which functions in DNA binding. The Per-Arnt-Sim (PAS) domain is required for the heterodimer between HIF-1α and HIF-1β. The oxygen-dependent degradation domain (ODD) has the proline residues at positions P402 and P562 for hydroxylation by Von Hippel-Lindau (VHL) protein and Lysine K532 for acetylation by arrest-defective-1 protein. Two transcriptional activation domains (TADs) which are necessary for the transactivation of target genes consist of the N-terminal TAD (N-TAD) and the C-terminal TAD (C-TAD). At the Asparagine position H802, factor inhibiting HIF-1α (FIH-1α) hydroxylates HIF-1α, as a result, inhibits HIF-1α activity. HIF-1β, on the other hand, consists of 789 amino acids, lacks the ODD and has only one TAD [10-12] (**Figure 1.2**).
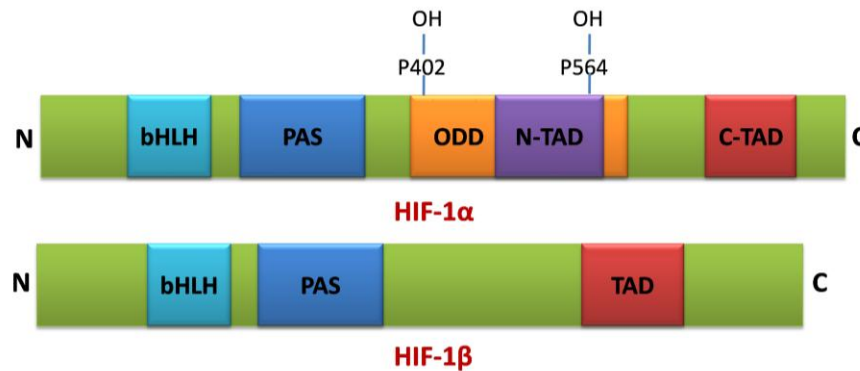

Figure 1.2. Schematic outline of the structure of HIF-1α and HIF-1β. HIF-1α and HIF-1β both possess a basis helix-loop-helix (bHLH) domain at the N-terminus allowing for the heterodimerization of HIF-1α and HIF-1β and a PAS domain, which is responsible for the DNA binding to the hypoxia responsive element (HRE). HIF-1α has two TAD domains allowing for binding to VHL and p300/CBP.

In human, HIF-1α and HIF-2α, which is also known as endothelial PAS domain protein 1 (ePAS1), share similar structure, function and regulatory pathway, whereas little is known about the regulation and function of HIF-3α (also known as IPAS). So far, at least five different splice variants may be expressed from the human HIF-3α that functions as an inhibitor of transcriptional responses to hypoxia [13].

2.2.   Oxygen-dependent mechanism of HIF-1α degradation

HIF-1α is specifically upregulated in hypoxia and rapidly degraded under conditions of atmospheric oxygen tension. This is largely understood in a mechanism involving regulations of protein stability via the ubiquitin pathway [14, 15].

Under normoxic conditions, prolyl hydroxylase (PHD) hydroxylases HIF-1α and allows it to interact with VHL protein complex which contains elongin-B (B), elongin-C (C), CUL2, RBX1 and a ubiquitin-conjugating enzyme (E2). Ubiquitin is guided by ubiquitin-activating enzyme (E1) to interact with E2 and then modifies HIF-1α. This modification leads to the degradation of HIF-1α in proteasome. Moreover, in the presence of oxygen, HIF is also hyroxylated by FIH-1 and this modification prevents the interaction between HIF-1α and CBP/p300 (cyclic AMP responsive element binding protein) to block the transcription of HIF-1-target genes. Since oxygen acts as a substrate for PHD2, HIF-1α is specifically accumulated within cells under hypoxic conditions. The accumulated HIF-1α, then translocates to the nucleus to heterodimer with HIF-1β and binds to the hypoxia responsive element (HRE) of the target genes which therefore induces the expression of several HIF-downstream genes [9] (**Figure 1.3**).
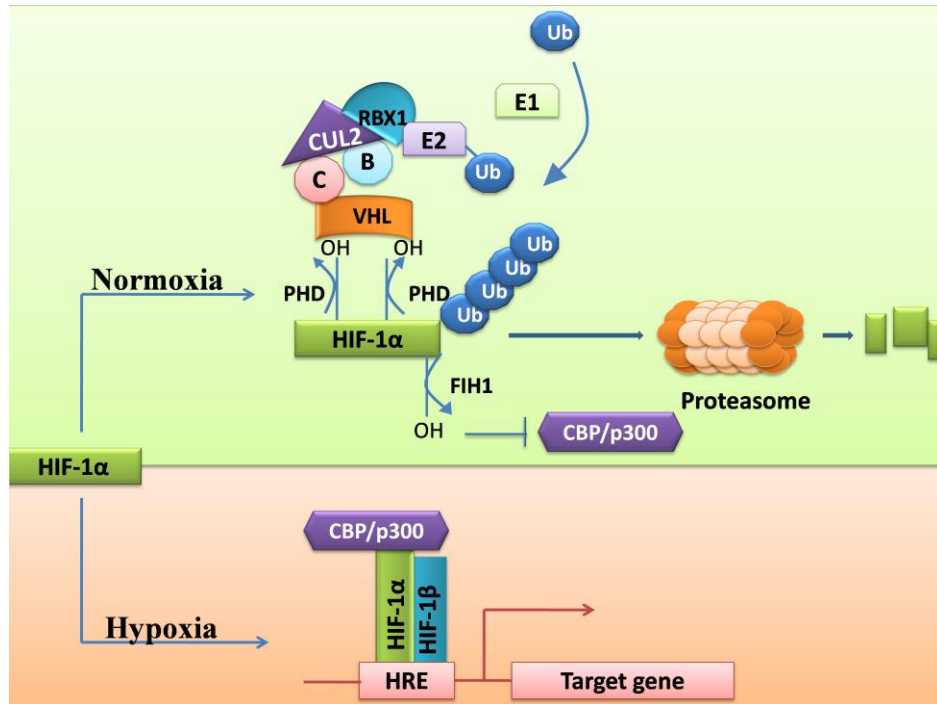
Figure 1.3. Oxygen-dependent degradation mechanism of HIF-1α. In normoxia, the cellular oxygen sensors (PHDs) hydroxylate specific proline residues (Pro-402 and Pro-564) of HIF-1α, leading to its proteosomal degradation mediated by VHL, an E3 ubiquitin ligase. In contrast, HIF-1α remains stable and functions under hypoxic conditions where it cooperates with its beta subunits and triggers the transcription of genes essential to adaptive responses to hypoxia.

2.3.   Oxygen-independent regulation of HIF-1α

Increasing evidence indicates that mechanisms other than pVHL-dependent HIF-1α degradation have an important role in controlling HIF-1α levels. Compared with pVHL, the regulation of these new pathways seems to be less dependent on oxygen availability and more on specific cellular conditions such as calcium or the presence of growth factors [16]. The receptor of activated protein C kinase (RACK1) has been identified to promote the O_2/PHD/VHL-independent and proteasome-dependent degradation of HIF-1α. RACK1 competes with heat shock protein HSP90 for binding to the PAS-A domain of HIF-1α and subsequently recruits Elongin-C, Elongin-B and other components of E3 ubiquitin ligase to HIF-1α [17]. The RACK1 pathway can also be regulated by calcium through the activity of calcineurin, a calcium- and calmodulin-dependent and serine/threonine-specific protein

phosphatase. Calcineurin dephosphorylates RACK1 in a calcium-dependent manner, thus blocks RACK1 dimerization and inhibits RACK1-mediated HIF-1α degradation [18].

The Phosphatidylinositol 3-kinase (PI3K)/Akt is also linked to HIF-1α protein degradation [19]. However, the modulation of the PI3K-Akt pathway and its role in HIF-1α regulation during hypoxia remains controversial and is highly context dependent. It has been suggested that the PI3K pathway might be activated by short-term hypoxia but inhibited by prolonged hypoxia [20, 21]. Glycogen synthase kinase 3 (GSK3), is phosphorylated and inactivated by Akt. GSK3β overexpression results in pVHL-independent HIF-1α ubiquitylation and proteasomal degradation via GSK3β- mediated HIF-1α phosphorylation [22]. Similarly, overexpression of forkhead box O4 (FOXO4) or constitutive activation of FOXO3α are also negatively regulated by Akt, also represses HIF-1a, the former by inducing pVHL-independent HIF-1α ubiquitylation and degradation [22] and the latter by inhibiting HIF-1α transactivation in a p300-dependent manner [23]. Hence, it is possible that prolonged hypoxia might inhibit the PI3K pathway, resulting in increased GSK3β activity and perhaps also FOXO4 and FOXO3α, which then results in decreased HIF-1α levels and activity.

In addition, reactive oxygen species (ROS) have been reported to be involved in regulation of HIF-1 protein level under normoxic and hypoxic conditions. Intracellular ROS are formed by reduction of oxygen and give rise to hydrogen peroxide (H_2O_2) and hydroxyl radicals [24]. Interestingly, accumulation of ROS has been shown to either increase stability or induce of the degradation of HIF. The proposed mechanism in which H_2O_2 stabilizes HIF has been reported to be involved in JunD, a member of the AP-1 transcriptional factor family. In *jun*D mutant cells, elevated H_2O_2 reduces the activity of PHDs thereby stabilizes HIFα [25]. Additionally, cytokine upregulation by ROS under normoxic conditions was also demonstrated to stabilize HIFα in other reports [26, 27]. In contrast, destabilization of HIF under hypoxic or normoxic conditions emphasizes the diversity of HIF's regulatory mechanism under different contexts [28, 29].

2.4.   Significance of HIF-1 in tumor growth and malignant progression

HIF-1 activates the transcription of a great number of genes that control adaptive responses to hypoxia. So far, more than 100 downstream genes regulated by HIF-1 have been characterized [7]. A recent study of global gene expression using DNA microarrays indicates that more than 2% of all human genes are directly or indirectly regulated by HIF-

1 in arterial endothelial cells [30]. The roles of HIF in hypoxic tumors are characterized in the followed functions:

Glucose and energy metabolism: It has been known for a hundred years that cancer cell metabolism is markedly different from that of the corresponding normal tissue cells. In 1920s, Otto Warburg first described the concept that glycolysis, i.e. the conversion of glucose to pyruvate and then to lactic acid in tumor tissue occurs even under normoxic conditions. In 1931, he was awarded the Nobel Prize in Physiology and Medicine for this discovery, which now is termed "Warburg effect" and so far is the best known about cancer cellular energy metabolism [31].

Warburg specified that differentiated tissue uses glycolysis to generate approximately 10% of the cell's ATP, while mitochondria accounts for 90%. In proliferative tissue and tumor, however, about 85% of the cellular energy is produced by glycolysis while the remainder is generated in the mitochondria. The increased glucose uptake which is required to maintain ATP production is a universal feature of cancer cells. This feature is used to detect cancerous tissues clinically by positron emission tomography (PET) flowing the administration of [^{18}F]-deoxyglucose [32]. This phenomenon occurs even when there is sufficient O_2 present to support mitochondrial function, and it is termed aerobic glycolysis. (**Figure 1.4**)
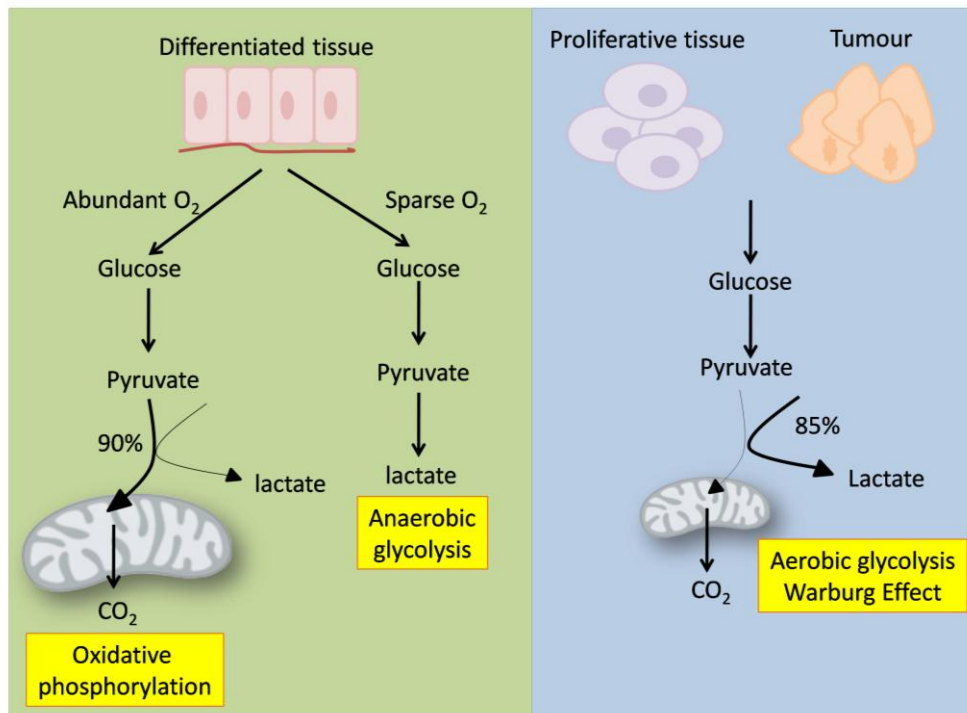
Figure 1.4. Schematic summarization about the differences of oxidative phosphorylation, anaerobic glycolysis and aerobic glycolysis (Warburg effect). In the presence of oxygen, differentiated tissues first metabolize glucose to pyruvate via glycolysis and then completely oxidize most of that pyruvate in the mitochondria to CO_2 during the process of oxidative phosphorylation. When oxygen is limited, cells can redirect the pyruvate generated by glycolysis away from mitochondrial oxidative phosphorylation by generating lactate (anaerobic glycolysis). On the other hand, cancer cells tend to convert most glucose to lactate regardless of oxygen status (aerobic glycolysis) [33].

The transcription factor HIF-1 has been implicated in regulating many of genes which are responsible for the metabolic shift [34, 35]. HIF-1 upregulates the transcription of glucose transporters GLUT1 and GLUT3 as well as hexokinase, the first enzyme of the Embden-Meyerhof (glycolytic) pathway together with a lot of glycolytic enzymes in order to increase glycolytic metabolism. HIF-1 suppresses the tricarboxylic acid (TCA) cycle by inducing pyruvate dehydrogenase kinase 1 (PDK1). Phosphorylation of E1 subunit of pyruvate dehydrogenase (PDH) by enzyme PDK-1 inactivates PHD activity, preventing the entry of pyruvate into the mitochondria and leads to pyruvate accumulation in the cytosol. The accumulated pyruvate is converted into lactate via lactate dehydrogenase (LDH) [36-38] (**Figure 1.5**).
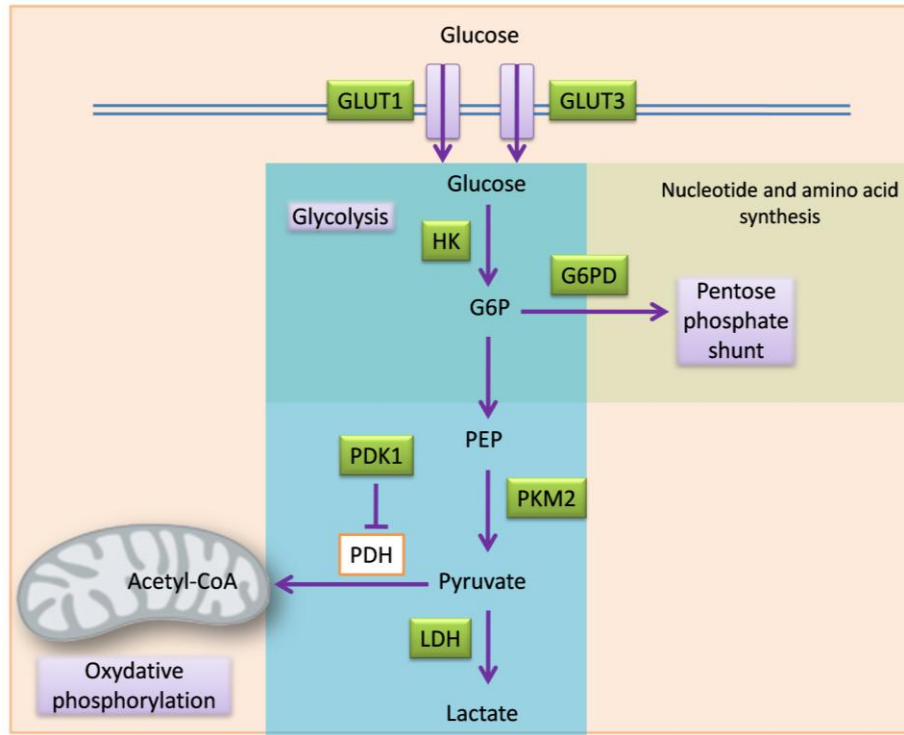
Figure 1.5. Brief overview of HIF-1α - mediated regulation of tumor cell metabolism. HIF-1 activation leads to an increase in several metabolic pathway including glycolysis and pentose phosphate pathways, meanwhile decreases the oxidative phosphorylation process. The enzymes which are upregulated by HIF-1 are labelled in green. GLUT: Glucose transporter, HK: Hexokinase, G6P: Glucose-6-phosphate, G6PD: Glucose-6-phosphate dehydrogenase PEP: Phosphoenolpyruvic acid, PKM2: Pyruvate kinase M2, PDH: Pyruvate dehydrogenase, PDK1: Pyruvate dehydrogenase kinase 1, LDH: Lactate dehydrogenase.

Vasculogenesis and angiogenesis: Vasculogenesis is the *de novo* formation of vasculature during embryonic development and also occurs in the organisms from circulating endothelial progenitor cells during tumor growth, revascularization following trauma, and so on. It refers to the movement of angiogenic progenitor cells to the sites of vascularisation and their differentiation afterward to become the beginning functioned vasculatures. On the other hand, angiogenesis terms the phenomenon of creating new capillary blood vessels from existing vessels [39]. Vascular endothelial cell growth factor (VEGF) involves intensively in both angiogenesis and vasculogenesis and is activated by HIF-1 together with a great number of angiogenic genes activated in hypoxia [40]. They include angiopoietin 1 (ANGPT1) and ANGPT2, placental growth factor (PGF) and

platelet-derived growth factor B (PDGFB). The regulation of angiogenesis by hypoxia is an important component of homeostatic mechanisms that link vascular oxygen supply to metabolic demand and the roles of HIF-1 in this regulation are well-characterized in a considerable number of reports [41-43].

Erythropoiesis, oxygen homeostasis and iron metabolism: In order to adapt to the shortage of oxygen, hypoxic cells tend to promote the erythropoiesis and iron metabolism. Several of the target genes of HIF are involved in iron homeostasis and erythropoiesis [44]. The discovery of erythropoietin (EPO), which is required for the formation of red blood cells and its interaction with HIF-1 clarifies the mechanism behind this phenomenon. However, *in vivo* and *in vitro* evidences suggest that HIF-2α but not HIF-1α is the key mediator in the overexpression of EPO. The iron metabolism is also increased in accordance to the higher requirement in the heme of the oxygen-binding proteins haemoglobin and myoglobin. HIF regulates proteins related to this process includes duodenal cytochrome b which transfers Fe^{3+} to Fe^{2+} ready for hemoglobin protein binding. Others proteins are divalent metal transporter 1 and transferrin, transferrin receptor which functions in transportation of iron molecules to the cells. [45, 46]

Cell proliferation and survival: Several growth factors, most notably insulin-like growth factor-2 (IGF2) and transforming growth factor-α (TGF-α) are HIF-1 target genes. Binding of these factors to their receptors, the insulin-like growth factor 1 receptor (IGF1R) and epidermal growth-factor receptor (EGFR), respectively increases translation of HIF-1α through PI3K/AKT/mTOR signalling pathway. Subsequently, HIF-1α triggers the expression of its target genes including IGF2 and TGF-α which induce cell proliferation and survival. HIF-1, therefore contributes to autocrine signalling pathways which are crucial for cancer progression. Increased cytokines and growth factors, and mutations of *RAS* and *RAF* oncogenes in many cancer cell types activate Mitogen-activated protein kinase (MAPK) and Phosphatidylinositol 3-kinase (PI3K) signalling pathways, which promote cell proliferation/ survival, also increase HIF-1α translation levels [9, 10, 47] (**Figure 1.6**).
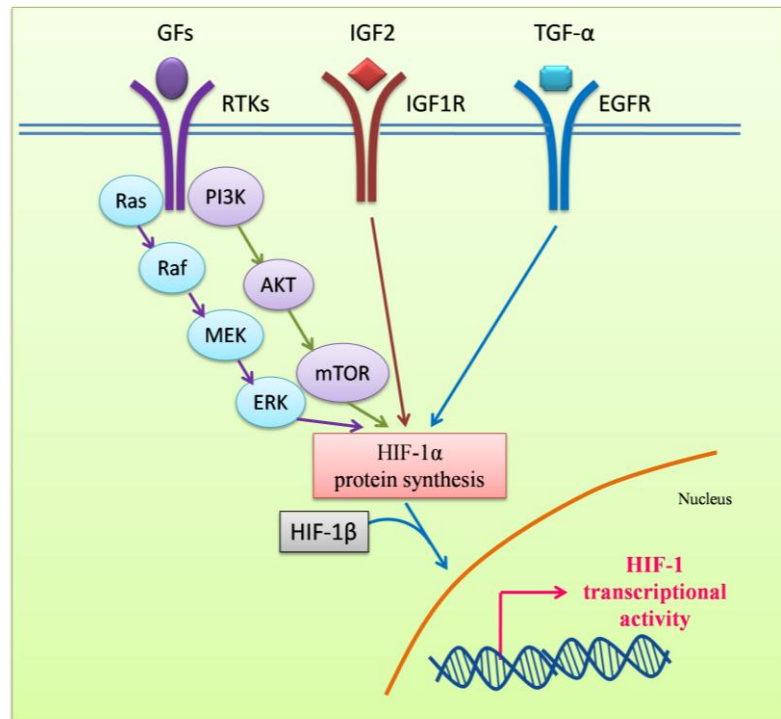
Figure 1.6. Interactions of HIF and other pathways relating to cell proliferation and survival. GFs: Growth factors, RTKs: Receptor tyrosine kinases, ERK: Extracellular-signal-regulated kinase, MAPK: Mitogen-activated protein kinase, MEK: MAPK/ERK kinase, PI3K: Phosphatidylinositol 3-kinase, mTOR: Mammalian target of Rapamycin. IGF2: Insulin-like growth factor-2, TGF-α: Transforming growth factor-α, IGF1R: Insulin-like growth factor 1 receptor, EGFR: Epidermal growth-factor receptor.

Apoptosis: Hypoxia has been shown to induce or suppress apoptosis in which HIF-1 plays a complex role. HIF-1α can induce apoptosis by stabilizing tumor suppressor gene p53. It has been shown that HIF-1α directly binds to the p53 ubiquitin ligase MDM2 both *in vivo* and *in vitro*, thereby stabilising p53 [48]. Hypoxia can upregulate HIF-downstream genes including pro-apoptotic genes *Bax* and *BNIP3*, *NIX* (a *BNIP3* homologue). Hypoxia also can cause growth arrest, which is mediated by p21 [49]. However, hypoxia can lighten the effect of apoptotic inducer in cells compared to the same treatment in normoxia [50]. In another report, HIF-1α can prevent apoptosis-induced by hypoxia in pancreatic cancer cell lines. Specifically, cells with high protein levels of HIF-1α in normoxia showed more resistance to apoptosis caused by hypoxia and glucose deprivation than cell lines with low HIF-1α expression [51]. In addition, the dominant

negative HIF-1α rendered pancreatic cancer cells sensitive to apoptosis and growth inhibition by hypoxia and glucose deprivation [52].

2.5.   Targeting hypoxic and HIF-active cancers

Since tumor hypoxia promotes malignant phenotypes and imposes disadvantages to standard therapies, several research groups have been focusing on strategies targeting tumor hypoxia to improve treatment outcomes. The strategies to design these drugs are based on the distinct characteristics of tumor hypoxia compared to normoxic counterparts. The most popular type of drugs that target tumor hypoxia is bioreductive prodrugs which are activated specifically under intracellular reductases within hypoxic cancer cells. These drugs employ one of five chemical moieties (nitro groups, quinines, aromatic *N*-oxides, aliphatic *N*-oxides and transition metals) [53]. PR-104 [54] and TH-302 [55] and Tirapazamine (TPZ) [56] are outstanding drugs in this group, which are currently progressing to clinical trials. These prodrugs are activated specifically by intracellular reductases within hypoxic cancer cells and then induce DNA break-down specifically under hypoxic conditions. On the other hand, oxygen within aerobic cells converts the toxic radical to original non-toxic compounds and thus imposes less cytotoxicity to the non-target tissues.

Another approach is directly targeting HIF's transcriptional activity by inhibition the interaction between HIF-1α and its coactivator p300/CREB. Suppressing HIF by antisense molecules and small inhibitors which directly bind to and inhibit HIF's activity are also promising approaches [57]. Other strategy such as increase of oxygen supply to solid tumors by administration of recombinant erythropoietin, a protein signalling molecule for red blood cell precursors in the bone marrow, thus increase oxygen supplement to anemia tissues [58] is also under investigated. Targeting vasculature network by anti-VEGF therapies using antibodies and small molecule receptor tyrosine kinase inhibitors are other approaches [59].

References

1. Vaupel, P., O. Thews, and M. Hoeckel, *Treatment resistance of solid tumors: role of hypoxia and anemia.* Med Oncol, 2001. **18**(4): p. 243-59.

2. Vaupel, P., *Hypoxia and aggressive tumor phenotype: implications for therapy and prognosis.* Oncologist, 2008. **13 Suppl 3**: p. 21-6.

3. Vaupel, P. and L. Harrison, *Tumor hypoxia: causative factors, compensatory mechanisms, and cellular response.* Oncologist, 2004. **9 Suppl 5**: p. 4-9.

4. Hockel, M. and P. Vaupel, *Tumor hypoxia: definitions and current clinical, biologic, and molecular aspects.* J Natl Cancer Inst, 2001. **93**(4): p. 266-76.

5. Moeller, B.J., R.A. Richardson, and M.W. Dewhirst, *Hypoxia and radiotherapy: opportunities for improved outcomes in cancer treatment.* Cancer Metastasis Rev, 2007. **26**(2): p. 241-8.

6. Shannon, A.M., et al., *Tumour hypoxia, chemotherapeutic resistance and hypoxia-related therapies.* Cancer Treatment Reviews, 2003. **29**(4): p. 297-307.

7. Ke, Q. and M. Costa, *Hypoxia-inducible factor-1 (HIF-1).* Mol Pharmacol, 2006. **70**(5): p. 1469-80.

8. Semenza, G.L., *Hypoxia-inducible factor 1: oxygen homeostasis and disease pathophysiology.* Trends Mol Med, 2001. **7**(8): p. 345-50.

9. Semenza, G.L., *Targeting HIF-1 for cancer therapy.* Nat Rev Cancer, 2003. **3**(10): p. 721-32.

10. Burrows, N., et al., *Hypoxia-inducible factor in thyroid carcinoma.* J Thyroid Res, 2011. **2011**: p. 762905.

11. Zagorska, A. and J. Dulak, *HIF-1: the knowns and unknowns of hypoxia sensing.* Acta Biochim Pol, 2004. **51**(3): p. 563-85.

12. Wang, G.L., et al., *Hypoxia-inducible factor 1 is a basic-helix-loop-helix-PAS heterodimer regulated by cellular O2 tension.* Proc Natl Acad Sci U S A, 1995. **92**(12): p. 5510-4.

13. Maynard, M.A., et al., *Dominant-negative HIF-3 alpha 4 suppresses VHL-null renal cell carcinoma progression.* Cell Cycle, 2007. **6**(22): p. 2810-6.

14. Begg, A.C., *Is HIF-1alpha a good marker for tumor hypoxia?* Int J Radiat Oncol Biol Phys, 2003. **56**(4): p. 917-9.

15. Semenza, G., *Signal transduction to hypoxia-inducible factor 1.* Biochem Pharmacol, 2002. **64**(5-6): p. 993-8.

16. Yee Koh, M., T.R. Spivak-Kroizman, and G. Powis, *HIF-1 regulation: not so easy come, easy go.* Trends Biochem Sci, 2008. **33**(11): p. 526-34.

17. Liu, Y.V. and G.L. Semenza, *RACK1 vs. HSP90: competition for HIF-1 alpha degradation vs. stabilization.* Cell Cycle, 2007. **6**(6): p. 656-9.

18. Liu, Y.V., et al., *Calcineurin promotes hypoxia-inducible factor 1alpha expression by dephosphorylating RACK1 and blocking RACK1 dimerization.* J Biol Chem, 2007. **282**(51): p. 37064-73.

19. Mottet, D., et al., *Regulation of hypoxia-inducible factor-1alpha protein level during hypoxic conditions by the phosphatidylinositol 3-kinase/Akt/glycogen synthase kinase 3beta pathway in HepG2 cells.* J Biol Chem, 2003. **278**(33): p. 31277-85.

20. Arsham, A.M., et al., *Phosphatidylinositol 3-kinase/Akt signaling is neither required for hypoxic stabilization of HIF-1 alpha nor sufficient for HIF-1-dependent target gene transcription.* J Biol Chem, 2002. **277**(17): p. 15162-70.

21. Stiehl, D.P., et al., *Normoxic induction of the hypoxia-inducible factor 1alpha by insulin and interleukin-1beta involves the phosphatidylinositol 3-kinase pathway.* FEBS Lett, 2002. **512**(1-3): p. 157-62.

22. Flugel, D., et al., *Glycogen synthase kinase 3 phosphorylates hypoxia-inducible factor 1alpha and mediates its destabilization in a VHL-independent manner.* Mol Cell Biol, 2007. **27**(9): p. 3253-65.

23. Emerling, B.M., et al., *PTEN regulates p300-dependent hypoxia-inducible factor 1 transcriptional activity through Forkhead transcription factor 3a (FOXO3a).* Proc Natl Acad Sci U S A, 2008. **105**(7): p. 2622-7.

24. Acker, T., J. Fandrey, and H. Acker, *The good, the bad and the ugly in oxygen-sensing: ROS, cytochromes and prolyl-hydroxylases.* Cardiovasc Res, 2006. **71**(2): p. 195-207.

25. Gerald, D., et al., *JunD reduces tumor angiogenesis by protecting cells from oxidative stress.* Cell, 2004. **118**(6): p. 781-94.

26. Haddad, J.J., *Recombinant human interleukin (IL)-1 beta-mediated regulation of hypoxia-inducible factor-1 alpha (HIF-1 alpha) stabilization, nuclear translocation and activation requires an antioxidant/reactive oxygen species (ROS)-sensitive mechanism.* Eur Cytokine Netw, 2002. **13**(2): p. 250-60.

27. Haddad, J.J. and S.C. Land, *A non-hypoxic, ROS-sensitive pathway mediates TNF-alpha-dependent regulation of HIF-1alpha.* FEBS Lett, 2001. **505**(2): p. 269-74.

28. Callapina, M., et al., *NO restores HIF-1alpha hydroxylation during hypoxia: role of reactive oxygen species.* Free Radic Biol Med, 2005. **39**(7): p. 925-36.

29. Liu, Q., et al., *A Fenton reaction at the endoplasmic reticulum is involved in the redox control of hypoxia-inducible gene expression.* Proceedings of the National Academy of Sciences of the United States of America, 2004. **101**(12): p. 4302-4307.

30. Manalo, D.J., et al., *Transcriptional regulation of vascular endothelial cell responses to hypoxia by HIF-1.* Blood, 2005. **105**(2): p. 659-69.

31.   Zhivotovsky, B. and S. Orrenius, *The Warburg Effect returns to the cancer stage.* Semin Cancer Biol, 2009. **19**(1): p. 1-3.

32.   Gatenby, R.A. and R.J. Gillies, *Why do cancers have high aerobic glycolysis?* Nat Rev Cancer, 2004. **4**(11): p. 891-9.

33.   Vander Heiden, M.G., L.C. Cantley, and C.B. Thompson, *Understanding the Warburg effect: the metabolic requirements of cell proliferation.* Science, 2009. **324**(5930): p. 1029-33.

34.   Denko, N.C., *Hypoxia, HIF1 and glucose metabolism in the solid tumour.* Nat Rev Cancer, 2008. **8**(9): p. 705-13.

35.   Iyer, N.V., et al., *Cellular and developmental control of O2 homeostasis by hypoxia-inducible factor 1 alpha.* Genes Dev, 1998. **12**(2): p. 149-62.

36.   Meijer, T.W., et al., *Targeting hypoxia, HIF-1, and tumor glucose metabolism to improve radiotherapy efficacy.* Clin Cancer Res, 2012. **18**(20): p. 5585-94.

37.   Semenza, G.L., *HIF-1 mediates the Warburg effect in clear cell renal carcinoma.* J Bioenerg Biomembr, 2007. **39**(3): p. 231-4.

38.   Upadhyay, M., et al., *The Warburg effect: insights from the past decade.* Pharmacol Ther, 2013. **137**(3): p. 318-30.

39.   Patan, S., *Vasculogenesis and angiogenesis as mechanisms of vascular network formation, growth and remodeling.* J Neurooncol, 2000. **50**(1-2): p. 1-15.

40.   Ferrara, N., *Molecular and biological properties of vascular endothelial growth factor.* J Mol Med (Berl), 1999. **77**(7): p. 527-43.

41.   Kelly, B.D., et al., *Cell type-specific regulation of angiogenic growth factor gene expression and induction of angiogenesis in nonischemic tissue by a constitutively active form of hypoxia-inducible factor 1.* Circ Res, 2003. **93**(11): p. 1074-81.

42.   Hirota, K. and G.L. Semenza, *Regulation of angiogenesis by hypoxia-inducible factor 1.* Crit Rev Oncol Hematol, 2006. **59**(1): p. 15-26.

43.   Pugh, C.W. and P.J. Ratcliffe, *Regulation of angiogenesis by hypoxia: role of the HIF system.* Nat Med, 2003. **9**(6): p. 677-84.

44.   Peyssonnaux, C., V. Nizet, and R.S. Johnson, *Role of the hypoxia inducible factors HIF in iron metabolism.* Cell Cycle, 2008. **7**(1): p. 28-32.

45.   Haase, V.H., *Hypoxic regulation of erythropoiesis and iron metabolism.* Am J Physiol Renal Physiol, 2010. **299**(1): p. F1-13.

46.   Yoon, D., et al., *Hypoxia-inducible factor-1 deficiency results in dysregulated erythropoiesis signaling and iron homeostasis in mouse development.* J Biol Chem, 2006. **281**(35): p. 25703-11.

47.   Gossage, L. and T. Eisen, *Alterations in VHL as potential biomarkers in renal-cell carcinoma.* Nat Rev Clin Oncol, 2010. **7**(5): p. 277-88.

48. Chen, D., et al., *Direct interactions between HIF-1 alpha and Mdm2 modulate p53 function.* J Biol Chem, 2003. **278**(16): p. 13595-8.

49. Greijer, A.E. and E. van der Wall, *The role of hypoxia inducible factor 1 (HIF-1) in hypoxia induced apoptosis.* J Clin Pathol, 2004. **57**(10): p. 1009-14.

50. Dong, Z., et al., *Apoptosis-resistance of hypoxic cells: multiple factors involved and a role for IAP-2.* Am J Pathol, 2003. **163**(2): p. 663-71.

51. Akakura, N., et al., *Constitutive expression of hypoxia-inducible factor-1alpha renders pancreatic cancer cells resistant to apoptosis induced by hypoxia and nutrient deprivation.* Cancer Res, 2001. **61**(17): p. 6548-54.

52. Chen, J., et al., *Dominant-negative hypoxia-inducible factor-1 alpha reduces tumorigenicity of pancreatic cancer cells through the suppression of glucose metabolism.* Am J Pathol, 2003. **162**(4): p. 1283-91.

53. Wilson, W.R. and M.P. Hay, *Targeting hypoxia in cancer therapy.* Nat Rev Cancer, 2011. **11**(6): p. 393-410.

54. Guise, C.P., et al., *The Bioreductive Prodrug PR-104A Is Activated under Aerobic Conditions by Human Aldo-Keto Reductase 1C3.* Cancer Research, 2010. **70**(4): p. 1573-1584.

55. Hu, J., et al., *Targeting the multiple myeloma hypoxic niche with TH-302, a hypoxia-activated prodrug.* Blood, 2010. **116**(9): p. 1524-7.

56. Brown, J.M., *SR 4233 (tirapazamine): a new anticancer drug exploiting hypoxia in solid tumours.* Br J Cancer, 1993. **67**(6): p. 1163-70.

57. Rapisarda, A., et al., *Identification of small molecule inhibitors of hypoxia-inducible factor 1 transcriptional activation pathway.* Cancer Res, 2002. **62**(15): p. 4316-24.

58. Dicato, M., et al., *Clinical benefit from erythropoietin.* Curr Opin Oncol, 2000. **12**(4): p. 297-302.

59. Lee, C.G., et al., *Anti-Vascular endothelial growth factor treatment augments tumor radiation response under normoxic or hypoxic conditions.* Cancer Res, 2000. **60**(19): p. 5565-70.

Chapter 2

Pancreatic cancer cell lines are resistant to chemotherapeutic drugs gemcitabine and TS-1 under hypoxic conditions

Abstract

Pancreatic cancer is one of the most lethal digestive system cancers with a 5-year survival rate of 4%–7%. Despite extensive efforts, recent chemotherapeutic regimens have provided only limited benefits to pancreatic cancer patients. Gemcitabine and TS-1, the current standard-of-care chemotherapeutic drugs for treatment of this severe cancer, have a low response rate. Hypoxic regions within pancreatic cancer with the consecutive activation of hypoxia inducible factor HIF are one of the factors responsible for the resistance of pancreatic cancer. To confirm the resistance of hypoxic cancer cells to the drugs gemcitabine and TS-1, I first examined the expression level of HIFs in human pancreatic cancer cell lines SUIT-2, CFPAC-1 and BxPC-3 and confirmed that all of these cell lines expressed both HIF-1α and HIF-2α proteins under reduced oxygen levels. Consequently, I concluded that these pancreatic cancer cell lines are resistance to gemcitabine and TS-1 treatments *in vitro* by low response rates of these drugs under hypoxic (1% O_2) and severe hypoxic (0.1% O_2) conditions compared to the response rate under normoxic condition (21% O_2). In addition, I found that multi-drug resistance-1 gene, which is one of the target genes of HIF-1, is involved in the resistance of these cell lines to gemcitabine and TS-1 under reduced oxygen conditions.

Introduction

Pancreatic cancer

Pancreas is an organ of the digestive system located deep in the upper part of the abdomen, having features of both endocrine and exocrine glands. Despite breakthroughs in cancer treatment, pancreatic cancer remains one of the most intractable solid tumors with a 5-year survival rate of 4%−7% in most reports [1, 2] and accounts for the fifth leading deadly cancer for both men and women [3]. During the last 4 decades, the 5-year survival rate of pancreatic cancer patients only improved from 2% to 6% [4]. Symptoms of pancreatic cancer including back pain, nausea, fatigue and weight loss, and thus, are indistinguishable with other common diseases and are often ignored, causing the pancreatic cancer incapable to be diagnosed in early stages. At the time of diagnosis, 70%−80% of patients have already progressed to locally advanced stage or metastatic disease. Histopathologically, most pancreatic cancers are characterized by severe desmoplasia that results from extensive production of extracellular matrix components by pancreatic stellate cells [5]. As a result, the pancreatic tumors are surrounded by a condensed desmoplastic layer and usually contain several regions with limited vasculature network and nutrition. The dense desmoplastic stroma can comprise up to 80% of pancreatic cancer tumor mass and often contains several hypoxic regions, which makes pancreatic cancer severely hypoxic compared to cancers derived from other parts of the human body [6] (**Figure 2.1**).
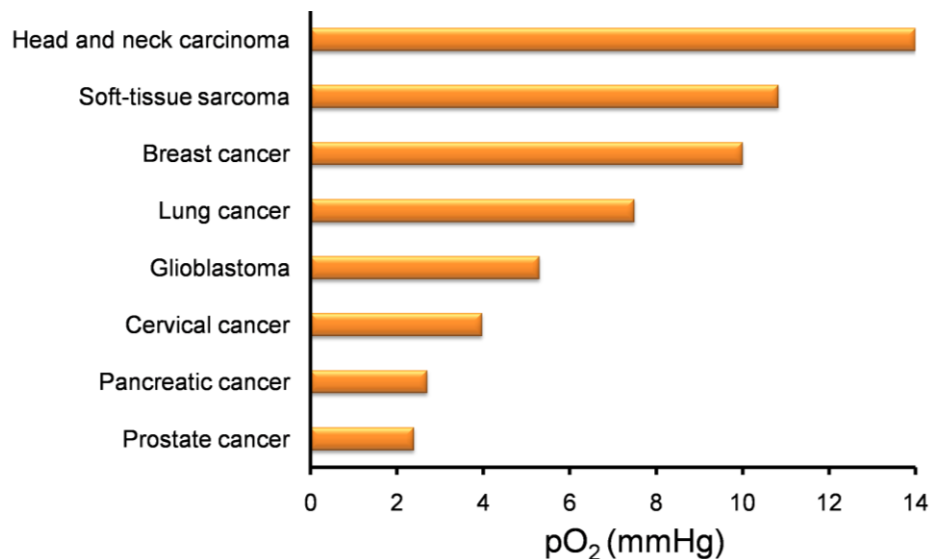
Figure 2.1: Pancreatic cancer is severely hypoxic compared to cancer derived from other parts of the human body. The graph was made from data summarized by Brown JM et al. (2004) [6]

In addition, genetic alterations of several oncogenes such as *KRAS*, *PTEN*, *SMAD4*, *AKT* and tumor suppressor genes such as *TP53*, *CDKN2A* are also responsible for the refractory and poor prognosis of pancreatic cancer [7]. As a result, the current therapeutics aiming to treat pancreatic cancer often results in limited outcomes. Current treatments for pancreatic cancer patients include resection, followed by adjuvant therapies including chemotherapies and radiation. Standard chemotherapeutic treatments for pancreatic cancer include gemcitabine, TS-1, paclitaxel, cisplatin, oxaliplatin, or capecitabine and combination treatments of these regiments in a hope to improve drugs' responses and extend survival rate of patients [8]. However, it has been reported that only 25-30% of patient response to the standard drugs gemcitabine and TS-1 [9].

Gemcitabine

Originally developed as an antiviral agent, gemcitabine was first studied in the late 1980s as a novel antimetabolite. Gemcitabine was approved by the US Food and Drug Administration (FDA) in 1996 for use in first line treatment of different stages of pancreatic adenocarcinomas. So far, gemcitabine have been emerging as a potential anticancer prodrug and is now used for a wide range of various solid tumors including non-small cell lung cancer, bladder cancer, breast cancer and pancreatic cancer and currently is being investigated in numerous trials as part of novel combination regimens [10].

Gemcitabine (2',2'-Difluoro-2'-Deoxycytidine, dFdC) is a nucleoside analog of deoxycytidine (**Figure 2.2**). It is a product of Eli Lilly and Company with the trade name Gemzar. As an antimetabolite, after administration, gemcitabine competes with deoxycytidine to inhibit DNA replication, therefore, leads to apoptosis of cells. Generally, cancer cells multiply more rapidly than healthy cells and therefore, are more sensitive to gemcitabine.
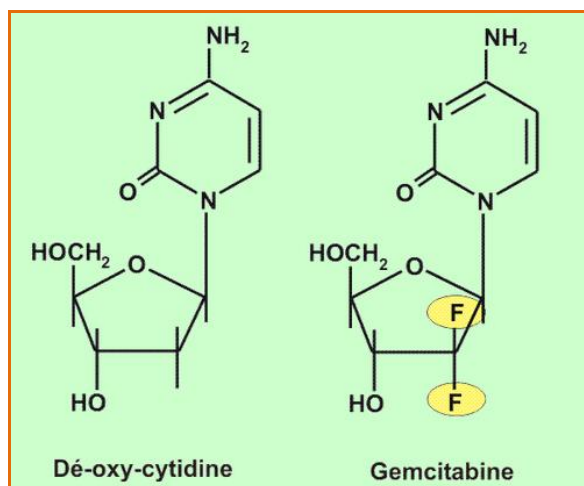
Figure 2.2. The structure of gemcitabine compared to cytidine

Gemcitabine is administered by intravenous route, since it is extensively metabolized by the gastrointestinal tract. Dose of gemcitabine ranges from 1-1.2 g/ m^2 of body surface area (BSA) according to the types of cancer treated as well as the current conditions of patients [11]. Since gemcitabine is a chemical drug, its side effects are often recognized. However, not everyone who takes the medication will experience side effects. The most frequently recorded side effects are flu-like symptoms, fever, fatigue, nausea, vomiting, poor appetite, skin rash, pain and low platelets in the blood. There are also other side effects which, however, do not often occur like diarrhea, bleeding, hair loss, mouth sores, drowsiness and blood in the urine [12].

As a nucleoside analog, gemcitabine is a prodrug that requires cellular uptake and intracellular phosphorylation in order to be activated. Once administered, gemcitabine is transported into cells by nucleoside transporters. It is then phosphorylated into gemcitabine monophosphate (dFdCMP) by deoxycytidine kinase (dCK), and dFdCMP is subsequently phosphorylated to gemcitabine diphosphate (dFdCDP) and gemcitabine triphosphate (dFdCTP) by nucleoside monophosphate (UMP/CMP) and nucleoside diphosphate kinase (NDK) [13]. There are three mechanisms of action of gemcitabine. First, gemcitabine diphosphate inhibits ribonucleotide reductase (RNR), which is the enzyme required for the transformation from cytidine diphosphate (CDP), a natural substrate in DNA replication to deoxycytidine diphosphate (dCDP). Therefore, the rate of incorporation of gemcitabine triphosphate to DNA during DNA replication increases. Second, gemcitabine allows one more nucleotide to pair before termination of the replication process. Thus, the gemcitabine nucleotide is less susceptible to repair by exonuclease enzymes, causing DNA repair

become more problematic. Third, gemcitabine is recognized as an agent with distinct self-potentiation: Gemcitabine preserves its own activity and durability by reducing deoxycytidine triphosphate inhibition of deoxycytidine kinase (which phosphorylates gemcitabine) and inhibiting deoxycytidine monophosphate deaminase (normally integral in gemcitabine degradation): Deoxycytidine monophosphate deaminase is inhibited directly by gemcitabine triphosphate and indirectly inhibited by gemcitabine diphosphate [14]. (**Figure 2.3**)

However, more than 90% of gemcitabine monophosphate is transformed to its inactive metabolite difluoro-deoxyuridine monophosphate *(*dFdUMP) which then is translocated outside of the cellular membrane. This process is taken place by cytidine deaminase (CD) and deoxycytidine monophosphate deaminase (DCTD) [13].
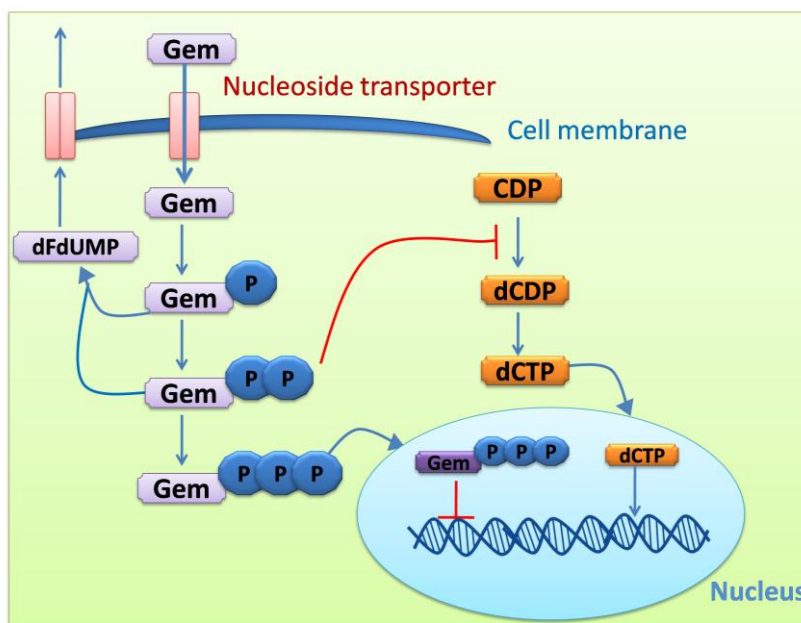

Figure 2.3. Mechanism of action of gemcitabine

TS-1 and its core drug 5-FU

5-FU (5-Fluorouracil) is an antimetabolite drug discovered in 1957 by Dushinsky et al. They realized that uracil is more preferably to integrate into tumor cells than other pyrimidine bases. Subsequently, they synthesized 5-FU in which hydrogen at fifth position in carbon backbone of uracil is substituted with fluorine to interfere with the nucleotide metabolism of cancer cells (**Figure 2.4**). At that time, 5-FU induced cytotoxicity

effectively to cancer cells. However, its adverse effects were also overwhelmed. They varied from nausea, vomiting and central nervous system disturbances making long term treatment difficult as well as unclear clinical effects. Therefore, improvements in administration way and 5-FU components were surveyed. In 1970, 5-FU was proposed to switch form intravenous to the oral route. During 20 years afterwards, two advanced modulators of 5-FU were gradually developed and improved. From 1991, after 5-FU and its 2 modulators CDHP and Oxo were combined in the ratio 1:0.4:1, a variety of preclinical studies and clinical trials were conducted and further made this combination become approved for several cancers. The first modulator, 5-chloro-2, 4-dihydroxypyridine (CDHP), enhances the pharmacological actions of 5-FU by potently inhibiting its degradation. The second modulator, potassium oxonate (Oxo), localizing in mucosal cells of the gastrointestinal (GI) tract after oral administration, reduces the incidence of GI toxicities by suppressing the activation of 5-FU in the GI tract. Thus, TS-1 combines FT, CDHP and Oxo at a molar ratio of 1:0.4:1 [15].
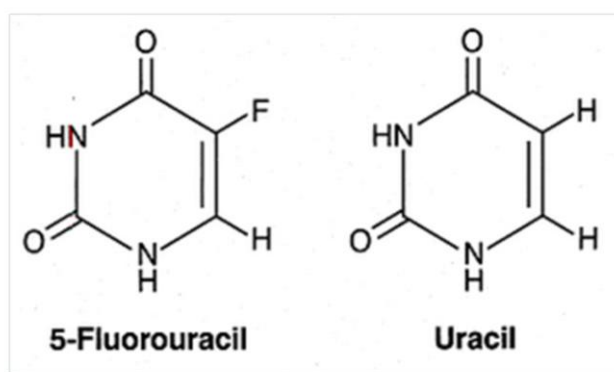

Figure 2.4. The structure of 5-FU compared to Uracil. 5-FU (5-Fluorouracil) is an analogue of the pyrimidine Uracil with the modification of 5th Hydrogen in the carbon backbone.

TS-1 has a wide variety of indications to extend the lives of numerous patients in Japan since it was released in 1999 by Taiho Pharmaceutical Co. Ltd. It is used for the treatment of gastric cancer, colorectal cancer, head and neck cancer, non-small cell lung cancer, inoperable or recurrent breast cancer, pancreas and biliary tract cancers. TS-1 was approved in Japan for seven kinds of cancer: gastric, colorectal, head and neck, non-small cell lung, unresectable or recurrent breast, pancreatic, and biliary tract cancers [16, 17].

Usually, the standard doses below are defined as the initial dose (single dose) for adults according to BSA as follows: BSA < 1.25 m^2, 80 mg/day; 1.25 m^2 < BSA <1.50 m^2,

100 mg/day; and 1.50 m^2 > BSA, 120 mg/day. TS-1 is administered twice daily, after breakfast and after the evening meal, for 28 consecutive days, followed by a 14-day rest. Since TS-1 is a chemical drug, its side effects are often recognized. However, not everyone who takes the medication will experience side effects. The common recorded side effects are leukopenia, neutropenia, thrombocytopenia, skin rash, diarrhea, vomiting, and stomatitis, etc. both in monotherapy and combination therapy [18].

After administration, 5-FU is transported into cell membranes by nucleoside transporters like other nucleotides. Within cells, 5-FU is phosphorylated to become fluorouridine monophosphate (FUMP). FUMP is then further phosphorylated to be fluorouridine diphosphate (FUDP) or fluorouridine triphosphate (FUTP). FUMP and FUDP can be converted to fluorodeoxyuridine diphosphate (FdUDP) and fluorodeoxyuridine triphosphate (FdTDP), respectively. FdUTP can compete with functional deoxynucleotides to inhibit DNA replication while FUTP antagonizes RNA synthesis. In another way, FdUMP can suppress thymidylate synthase (TS), an important enzyme which converses deoxyuridine monophosphate (dUMP) to deoxythymidine monophosphate (dTMP) and plays an important role in DNA repair. Thus, by inhibiting TS, 5-FU limits the precursor for DNA synthesis and further induces toxicity to cells. However, 5-FU also expresses high level of drug resistance. Up to 80% of administered 5-FU is broken down by dihydropyrimidine dehydrogenase (DPD) to the inactivated form dihydrofluorouracil (DHFU) in the liver (**Figure 2.5**) [19, 20].

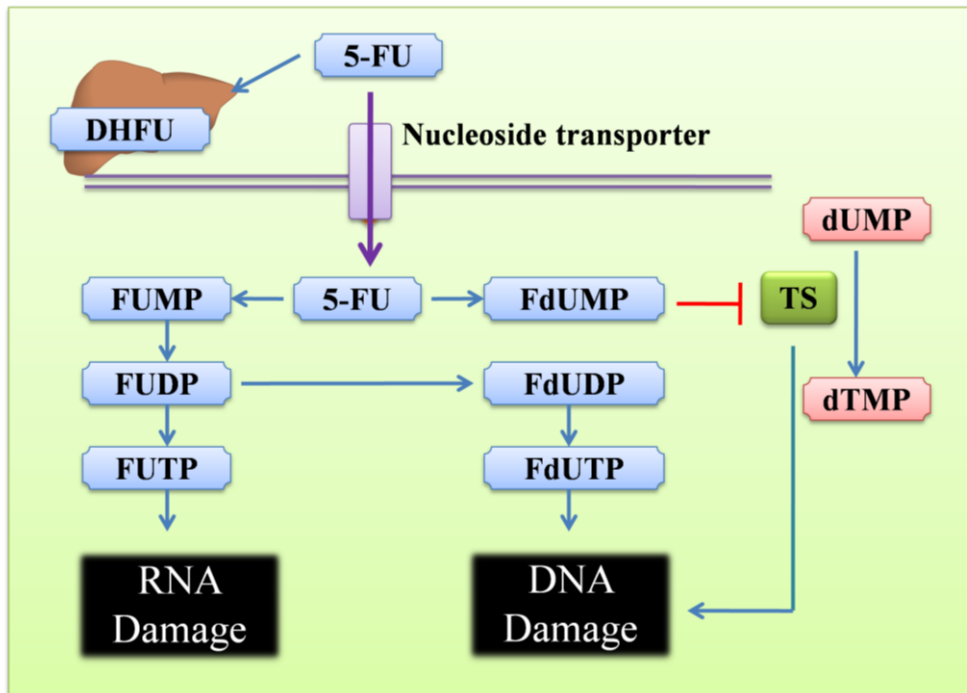**Figure 2.5**. TS-1 mechanism of action. TS-1 induces cell death by three smechanisms. The dysfunctioned products of 5-FU: fluorouridine triphosphate (FUTP) and fluorodeoxyuridine triphosphate (FdTDP) compete with functional nucleotides to trigger RNA and DNA damages, respectively. 5-FU also suppresses thymidylate synthase (TS), thereby restricts deoxythimidine which is necessary for DNA synthesis and further impairs DNA repair.

Materials and Methods

Western blot

SUIT-2 human pancreatic cancer cells were purchased from the Japanese Cancer Research Resource Bank (Osaka, Japan) and maintained in DMEM (Life Technologies, Carlsbad, CA, USA) supplemented with 5% FBS, penicillin (100 units /mL) and streptomycin (100 μg /mL) (Nacalai Tesque, Kyoto, Japan) in a multigas incubator (Sanyo, Osaka, Japan). CFPAC-1 and BxPC-3 pancreatic cancer cells were kindly received from National Cancer Institute and they were cultured in IMDM (Sigma-Aldrich, St. Louis, MO) and RPMI (Thermo Fisher Scientific, Waltham, MA, USA) media supplemented with 10% FBS and antibiotics at the above concentration. These pancreatic cancer cells were seeded at 1×10^5 cells on 6-well plates, pre-incubated for 12 hours in normoxia and further cultured in hypoxia at 37^oC, 1% O_2, 5% CO_2 for 24 hours. The cell lysate was collected after directly added with 200 μL 2 × sample buffer. The samples were then heated at 95^oC, centrifuged at room temperature at 10,000 × g, and vortexed for 5 minutes in each step. 20 μL of prepared samples was applied to 10% SDS-PAGE gel and run at 200 mA, 150V, 90 minutes (constant voltage).

Discontinuous buffers (I: 80% 375 mM Tris-HCl pH 10.4 + 10% methanol, II: 80% 25 mM Tris-HCl pH 10.4 + 10% methanol, III: 80% 25 mM Tris-HCl pH 9.4, 40 mM 6-amino hexa acid + 10% methanol) was used for transferring the proteins from the SDS-PAGE gel to nitrocellulose membranes by the settings of 200 mA, 20V, 60 minutes (constant voltage). The membrane then was washed by TBST 5 minutes for 3 times, and blocked with 5% skim milk in TBST for 1 hour at room temperature. The binding of primary antibody and secondary antibody to the membrane were carried on overnight at 4^0C and 1 hour at room temperature, respectively. The membrane was washed by TBST 5 minutes for 3 times and detected by LAS 4000 (Fujifilm, Tokyo, Japan) after adding ECL Prime Western Blotting Detecting reagent (GE Healthcare, Little Chalfont, UK). Before and after the addition of primary and secondary antibody, the membrane was washed by TBST 5 minutes for 3 times. All the used antibodies are diluted at 1/1000 ratio and they are listed in **Table 2.1**.

Table 2.1: Antibodies used in Western blot experiments.

	Antibody name	Company	Product code
1st antibody	Anti-Actin mouse monoclonal Ab	Sigma-Aldrich	A4700
	Anti-HIF-1α rabbit polyclonal Ab	Novus Biologicals	A NB100-149
	Anti-HIF-2α rabbit polyclonal Ab	Novus Biologicals	NB100-149
	Anti MDR-1 rabbit polyclonal Ab	Santa Cruz	H-241
2nd antibody	Anti-mouse IgG HRP-linked Ab	Cell Signaling Technology	#7076
	Anti-rabbit IgG HRP-linked Ab	Cell Signaling Technology	#7074

WST-1 proliferation assay

Cells were seeded at a density of 2×10^3 cells/well in 96-well plates and pre-incubated for 12 hours in normoxia. TS-1 (Taiho, Tokyo, Japan) and gemcitabine (Fluorochem, Derbyshire, UK) were added to the medium as a dilution series of 0–1,000 μM and 0–100 nM, respectively, before incubation in 21%, 1%, or 0.1% O_2. After incubation for 72 hours, 10 μL of WST-1 reagent (Roche Diagnostics, Indianapolis, IN, USA) was added to each well. The cells were seeded at 2×10^3 cells in 100 μL DMEM/ 5% FCS in 96-well plate and pre-incubated for 12 hours in normoxia. After a 3-hour incubation in normoxia, the OD (450 nm) of each well was measured with the reference OD (750 nm) using a microplate reader Model 680XR (Bio-Rad, Hercules, CA, USA).

Calcein AM proliferation assay

Cells were seeded at 1×10^3 cells in 96-well plates and preincubated overnight in normoxia. Immediately after addition of 100, 10, 1, or 0 μM 5-FU (Sigma–Aldrich) or 10, 5, 1, 0 nM gemcitabine, the plates were incubated under 21%, 1%, or 0.1% O_2 conditions for 72 hours. The cells were washed with 100 μL $1 \times$ DW (dilute/wash) buffer (Trevigen, Gaithersburg, UK), which was replaced with new DW buffer containing 1 μM calcein AM. The plates were then incubated in normoxia for 30 minutes and the fluorescence intensity was measured using an Infinite® F500 (Tecan, Männedorf, Switzerland) with excitation/emission of 485 nm/535 nm.

Results

Expression of HIFs in pancreatic cancer cell lines

HIF-1α has been shown to be overexpressed in several pancreatic cancer cell lines in hypoxic conditions and tumor models [21]. However, the expression of HIF-2α in these cell lines has not been investigated. In this study, I induced hypoxic condition with 1% O_2 or 0.1% O_2 for SUIT-2, CFPAC-1, BxPC-3 pancreatic cancer cell lines and observed the significant upregulation of HIFs protein by hypoxic treatments (**Figure 2.6**). Thus, it is likely that the adaptation to hypoxic stress of these pancreatic cancer cells lines is regulated by both HIF-1α and HIF-2α activity.
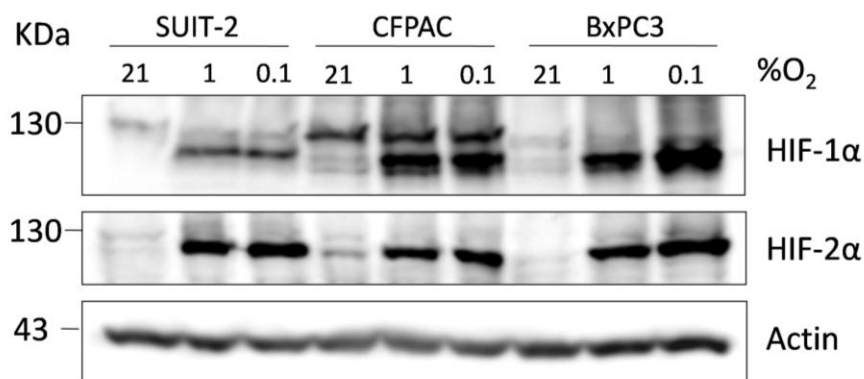

Figure 2.6. Western blot showing the overexpression of HIF-1α and HIF-2α proteins under hypoxic induction with 1% O_2 and 0.1% O_2 for 24 hours.

Resistance of pancreatic cancer cell lines to chemotherapeutic drugs

Gemcitabine and 5-FU have been proven to be effective in cell death induction and growth inhibition of several pancreatic cancer cell lines including AsPC-1, Capan-1, Mia PaCa-2 and T3M4 [22], BxPC-3, and CFPAC-1 and SUIT-2 [23] with different responses to the drug. Firstly, I examined the sensitivity of SUIT-2, with gemcitabine and 5-FU under normoxic (21% O_2), hypoxic (1% O_2) and severe hypoxic conditions (0.1% O_2). The sensitivity of the cells to drugs were examined by both WST-1 and Calcein AM proliferation assays (**Figure 2.7**). The effect of gemcitabine was influenced by only the hypoxic (1% O_2) treatment (**Fig. 2.7a, b),** whereas the effect of 5-FU was influenced by severe hypoxic conditions (**Fig. 2.7c, d**).
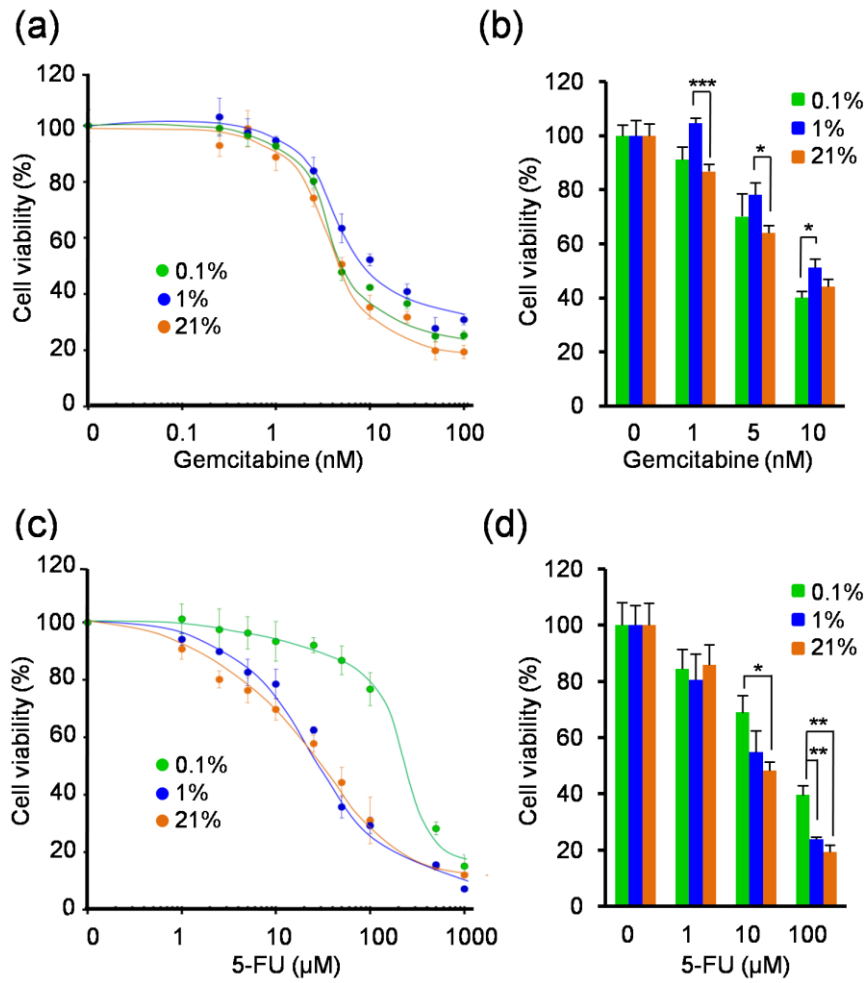
Figure 2.7: Responses of SUIT-2 to the chemotherapeutic drugs gemcitabine and TS-1 by WST-1 assay (**a** and **c**) and Calcein AM (**b** and **d**) under normoxic (21% O_2), hypoxic (1% O_2) and severe hypoxic condition (0.1% O_2) after 72 hours of treatment, n = 4 or 5.

In addition to SUIT-2 cells, I also evaluate the effects of hypoxic treatments on CFPAC-1 and BxPC-3 to the drugs. Since both WST-1 and Calcein AM assays give consistent results for SUIT-2 cells, I applied only WST-1 for the the evaluation with CFPAC-1 and BxPC-3 (**Figure 2.8**).
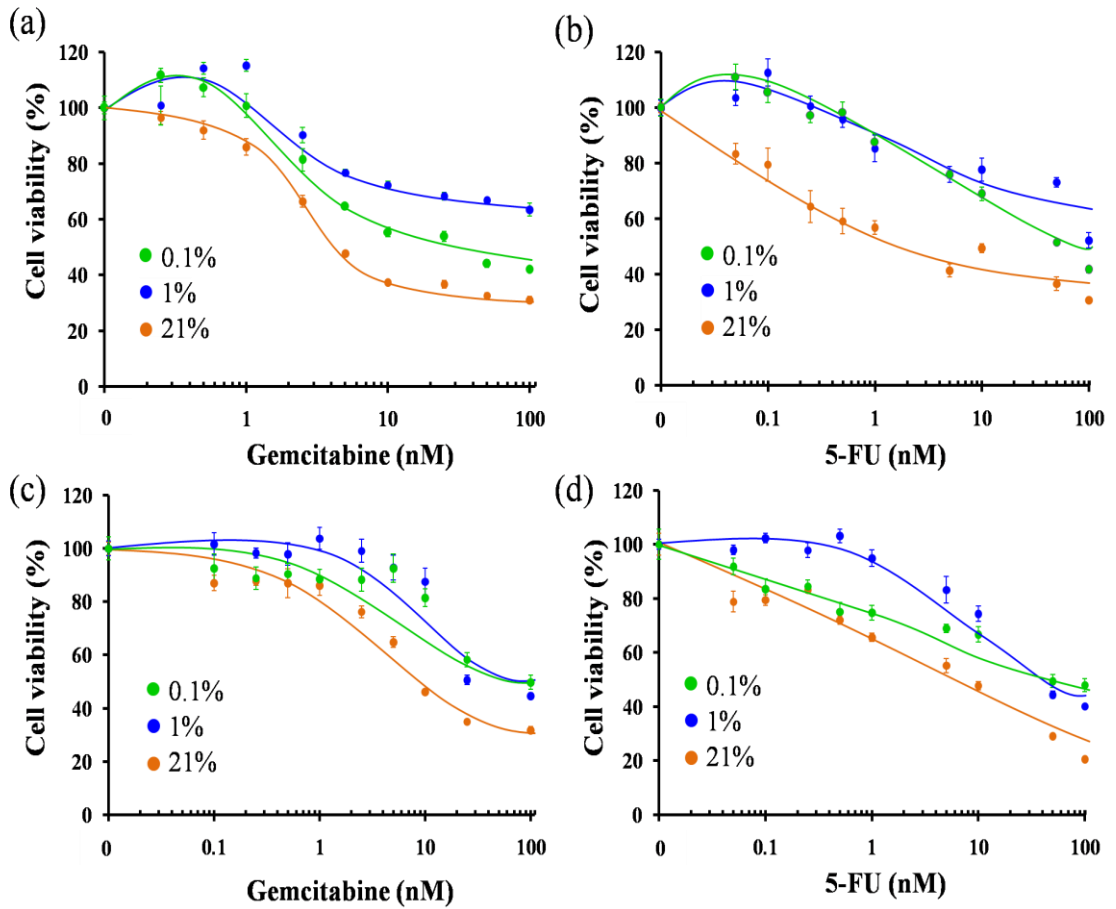
Figure 2.8: Responses of CFPAC-1 (**a** and **b**) and BxPC-3 (**c** and **d**) to the chemotherapeutic drugs gemcitabine and TS-1 by WST-1 assay under normoxic and hypoxic condition after 72 hours of treatment, n = 4 or 5.

By using a variety of gemcitabine and 5-FU doses in a serial dilution, I confirmed the effects of gemcitabine and 5-FU on pancreatic cancer cells in a dose-dependent manner. Notably, all of these pancreatic cancer cells showed lower sensitivity to the drugs under hypoxic and severe hypoxic conditions as compared to normoxic conditions. The half maximal inhibitory concentration (IC_{50}) of the drugs on the cell lines under each condition are shown in **Table 2.2**. These results suggest that hypoxic conditions trigger the cell resistance to these chemotherapeutic drugs.

Table 2.2: Half maximal inhibitory concentration (IC_{50}) values) showing responsibility of each cell lines to gemcitabine (nM) and 5-FU (μM) in normoxic and hypoxic conditions.

		Normoxia (21%)	Hypoxia (1%)	Severe hypoxia (0.1%)
Gemcitabine (nM)	SUIT-2	4.8	10.1	4.8
	CFPAC-1	4.1	>100	37.6
	BxPC-3	8.9	79.8	80.2
5-FU (μM)	SUIT-2	38.1	38.4	280
	CFPAC-1	1.9	>100	90.8
	BxPC-3	6.3	37.8	39.9

MDR-1 is a downstream gene of HIFs and involve in drugs resistance of SUIT-2 cell line

Multidrug resistance (*MDR-1*) has been reported as a gene directly regulated by HIF-1 and be associated with chemotherapeutic drug resistance. A HIF-1 binding site in *MDR-1* gene promoter has been identified [24]. I observe a slight upregulation of MDR-1 protein under hypoxic condition (1% O_2) and the significant upregulation of MDR-1 protein under severe hypoxic condition (0.1% O_2). Of note, the hypoxia-induction of *MDR-1* gene only remarkable occurs under treatment with gemcitabine and 5-FU and this induction was well-correlated with the dose of treatments (**Figure 2.9**), suggesting that the resistance of SUIT-2 to 5-FU and gemcitabine is likely to be moderated by *MDR-1* gene.
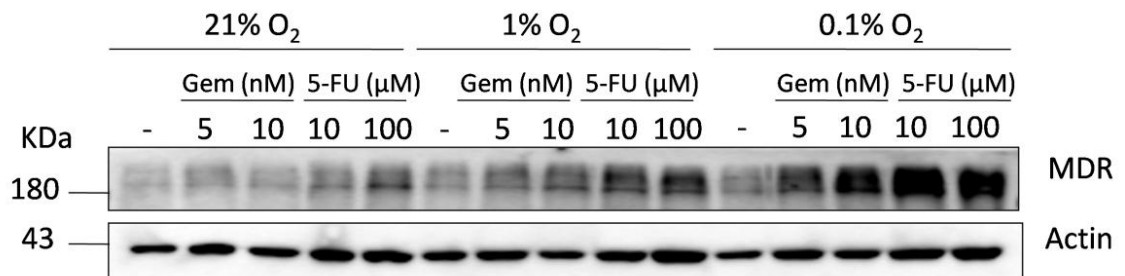

Figure 2.9: MDR-1 proteins are highly overexpressed under treatment with gemcitabine and 5-FU in hypoxia.

Discussion

Gemcitabine and TS-1 are among the most advanced drugs for treatment of pancreatic cancers and currently are widely used to treat a variety of cancers. Treatment of cells with the anti-metabolite drugs gemcitabine and TS-1 causes DNA and RNA damages, which in turn affects cell proliferation and survival. I conducted both WST-1 and calcein AM viability assays to exclude the possibility that reliability of the WST-1 assay was affected by impairment of mitochondria after long-term incubation in hypoxia, as reported in other cell lines [25] Overall, both assays gave consistent results with similar resistance patterns for each drug under hypoxic conditions. My inhibition results of gemcitabine and 5-FU were highly consistent with previous reports about the effect of gemcitabine and TS-1 on these cell lines [23, 26, 27]. I observed the proliferation inhibition effects of gemcitabine and TS-1 significantly in normoxic cells whereas the cells in hypoxic and/or severe hypoxic conditions develop resistance to them (**Figure 2.7, 2.8** and **Table 2.2)**. These results can be interpreted by the fact that severe hypoxic cancer cells tend to terminate DNA synthesis, thus, effect of TS-1 which is based on DNA and RNA damages cannot be achieved in this condition. In addition, resistance of pancreatic cancer cells to these drugs under hypoxic conditions is often observed, with the proposed mechanism involving PI3K/Akt/NF-kB or mTOR pathways [28, 29]. In this study, I observed the upregulation of MDR-1, a downstream gene of HIF under reduced oxygen levels. MDR-1 is a plasma-membrane-located glycoprotein which confers drug resistance by actively pump several compounds outside cells [30]. Thus, it is likely that the resistance of these cells to the drugs is mediated by MDR-1. In my study, the lower resistance of SUIT-2 to gemcitabine in severe hypoxia (0.1% O_2) than in milder hypoxia (1% O_2) was described for the first time, and the underlying mechanism is under investigation.

References

1.   Lemke, J., et al., *Survival and prognostic factors in pancreatic and ampullary cancer.* Anticancer Res, 2014. **34**(6): p. 3011-20.

2.   Kleeff, J., et al., *Pancreatic cancer: from bench to 5-year survival.* Pancreas, 2006. **33**(2): p. 111-8.

3.   Siegel, R.L., K.D. Miller, and A. Jemal, *Cancer statistics, 2016.* CA Cancer J Clin, 2016. **66**(1): p. 7-30.

4.   Siegel, R., et al., *Cancer statistics, 2014.* CA Cancer J Clin, 2014. **64**(1): p. 9-29.

5.   Apte, M.V., et al., *Desmoplastic reaction in pancreatic cancer: role of pancreatic stellate cells.* Pancreas, 2004. **29**(3): p. 179-87.

6.   Brown, J.M. and W.R. Wilson, *Exploiting tumour hypoxia in cancer treatment.* Nat Rev Cancer, 2004. **4**(6): p. 437-47.

7.   Bardeesy, N. and R.A. DePinho, *Pancreatic cancer biology and genetics.* Nat Rev Cancer, 2002. **2**(12): p. 897-909.

8.   Chiorean, E.G. and A.L. Coveler, *Pancreatic cancer: optimizing treatment options, new, and emerging targeted therapies.* Drug Des Devel Ther, 2015. **9**: p. 3529-45.

9.   Sheikh, R., et al., *Challenges of drug resistance in the management of pancreatic cancer.* Expert Rev Anticancer Ther, 2010. **10**(10): p. 1647-61.

10.   Barton-Burke, M., *Gemcitabine: a pharmacologic and clinical overview.* Cancer Nurs, 1999. **22**(2): p. 176-83.

11.   Song, H., et al., *Phase II trial of gemcitabine and S-1 for patients with advanced pancreatic cancer.* Cancer Chemother Pharmacol, 2013. **72**(4): p. 845-52.

12.   Eyre, T.A., et al., *Gemcitabine-induced large vessel vasculitis demonstrated by PET CT: a rare, important side effect.* Int J Hematol, 2014. **99**(6): p. 798-800.

13.   de Sousa Cavalcante, L. and G. Monteiro, *Gemcitabine: metabolism and molecular mechanisms of action, sensitivity and chemoresistance in pancreatic cancer.* Eur J Pharmacol, 2014. **741**: p. 8-16.

14.   Ueno, H., K. Kiyosawa, and N. Kaniwa, *Pharmacogenomics of gemcitabine: can genetic studies lead to tailor-made therapy?* Br J Cancer, 2007. **97**(2): p. 145-51.

15. Shirasaka, T., *Development history and concept of an oral anticancer agent S-1 (TS-1): its clinical usefulness and future vistas.* Jpn J Clin Oncol, 2009. **39**(1): p. 2-15.

16. Okamoto, I. and M. Fukuoka, *S-1: a new oral fluoropyrimidine in the treatment of patients with advanced non-small-cell lung cancer.* Clin Lung Cancer, 2009. **10**(4): p. 290-4.

17. Kinoshita, T., et al., *Phase II trial of S-1 for neoadjuvant chemotherapy against scirrhous gastric cancer (JCOG 0002).* Gastric Cancer, 2009. **12**(1): p. 37-42.

18. Ueno, H., et al., *Randomized phase III study of gemcitabine plus S-1, S-1 alone, or gemcitabine alone in patients with locally advanced and metastatic pancreatic cancer in Japan and Taiwan: GEST study.* J Clin Oncol, 2013. **31**(13): p. 1640-8.

19. Longley, D.B., D.P. Harkin, and P.G. Johnston, *5-fluorouracil: mechanisms of action and clinical strategies.* Nat Rev Cancer, 2003. **3**(5): p. 330-8.

20. West, C.M., T. Jones, and P. Price, *The potential of positron-emission tomography to study anticancer-drug resistance.* Nat Rev Cancer, 2004. **4**(6): p. 457-69.

21. Zhao, T., et al., *Inhibition of HIF-1alpha by PX-478 enhances the anti-tumor effect of gemcitabine by inducing immunogenic cell death in pancreatic ductal adenocarcinoma.* Oncotarget, 2015. **6**(4): p. 2250-62.

22. Shi, X., et al., *Acquired resistance of pancreatic cancer cells towards 5-Fluorouracil and gemcitabine is associated with altered expression of apoptosis-regulating genes.* Oncology, 2002. **62**(4): p. 354-62.

23. Halloran, C.M., et al., *5-Fluorouracil or gemcitabine combined with adenoviral-mediated reintroduction of p16INK4A greatly enhanced cytotoxicity in Panc-1 pancreatic adenocarcinoma cells.* J Gene Med, 2004. **6**(5): p. 514-25.

24. Comerford, K.M., et al., *Hypoxia-inducible factor-1-dependent regulation of the multidrug resistance (MDR1) gene.* Cancer Res, 2002. **62**(12): p. 3387-94.

25. Weir, L., et al., *The reduction of water-soluble tetrazolium salt reagent on the plasma membrane of epidermal keratinocytes is oxygen dependent.* Anal Biochem, 2011. **414**(1): p. 31-7.

26. Arumugam, T., et al., *Epithelial to mesenchymal transition contributes to drug resistance in pancreatic cancer.* Cancer Res, 2009. **69**(14): p. 5820-8.

27.   Wu, H.W., et al., *Intrinsic chemoresistance to gemcitabine is associated with constitutive and laminin-induced phosphorylation of FAK in pancreatic cancer cell lines.* Molecular Cancer, 2009. **8**.

28.   Yokoi, K. and I.J. Fidler, *Hypoxia increases resistance of human pancreatic cancer cells to apoptosis induced by gemcitabine.* Clin Cancer Res, 2004. **10**(7): p. 2299-306.

29.   Yoshiba, S., et al., *Hypoxia induces resistance to 5-fluorouracil in oral cancer cells via G(1) phase cell cycle arrest.* Oral Oncol, 2009. **45**(2): p. 109-15.

30.   Ueda, K., et al., *Expression of a full-length cDNA for the human "MDR1" gene confers resistance to colchicine, doxorubicin, and vinblastine.* Proc Natl Acad Sci U S A, 1987. **84**(9): p. 3004-8.

Chapter 3

Evaluation of the efficacy of TOP3 *in vitro*

Abstract

In **Chapter 2**, I confirmed the resistance of pancreatic cancer cells to standard chemotherapeutic drugs gemcitabine and TS-1 under reduced oxygen levels. That result motivated me to evaluate the cytotoxic effects of TOP3 when it is treated to the hypoxic pancreatic cancer cells. I examined the effects of TOP3 on a pancreatic cancer line SUIT-2 under tumor hypoxia-mimic (reduced oxygen and nutrition) conditions. TOP3 was purified from *E. coli* SoluBL21™ Competent cells and SUIT-2 cells was treated with TOP3 under hypoxic conditions with starved medium (1% O_2, 1% FBS, 500 mg/mL glucose) or severe hypoxic conditions with starved medium (0.1% O_2, 0.1% FBS, 100 mg/mL glucose). Compared to the untreated control samples, TOP3 significantly induced cell death under hypoxic conditions as indicated by an increase in sub-G1 fraction detected by flow cytometry analysis. The cell death induction was completely abolished in samples treated under norrmoxic condition, suggesting the specificity and treatment efficiency of TOP3 to hypoxic cancer cells.

Introduction

Protein transduction domains (PTDs)

Protein transduction domains (PTDs), also termed cell permeable proteins or membrane translocating sequences are small peptides that are able to ferry much larger molecules into cells independent of classical endocytosis. This property makes PTDs ideal tools to transfer proteins and other molecules into living cells for research purposes [1].

PTDs can be derived from a variety of sources of origin such as virus, *Drosophila*, and human. The HIV-1 transactivator of transcription (TAT) and the HSV-1 VP22 protein are the best characterized viral PTDs. Other homeodomains PTDs from *Drosophila* have been also extensively studied *in vitro* and *in vivo*. Several other peptides have been synthesized in attempt to create more potential PTDs and to elucidate the mechanism by which PTDs transport proteins across cell membranes. Human derived PTDs may overcome immunogenicity problems arising when treating with virus derived fusion proteins such as TAT or VP22. The summarization of most applicable PTDs is listed in **Table 3.1**.

Table 3.1: Properties of some reported PTDs

Origin	Name	Sequence	References
HIV-1	TAT	YGRKKRRQRRR	[2-4]
HSV-1	VP22	DAATATRGRSAASRPTERPRAPARSASRPRRPVD	[5, 6]
Drosophila	penetratin	RQIKIWFQNRRMKWKK	[7]
Drosophila	Ftz Fushi tarazu	RQIKIWFQNRRMKSKK	[8]
Human	Hox-A5	RQIKIWFQNRRMKWKK	[9]
Human	IsL-1	RVIRVWFQNKRCKDKK	[10, 11]
Synthetic PTD	PTD-3	KKKKKKKKKETWWETWWTEW	[12]
Synthetic PTD	PTD-4	YARAAARQARA	[13]
Synthetic PTD	PTD-5	RRQRRTSKLMKR	[14]
Synthetic PTD	L-R9	RRRRRRRRR	[2]
Synthetic PTD	Transportan	GWTLNSAGYLLGKINLKALAALAKKIL	[15]
Synthetic PTD	Peptide 2	SGWFRRWKK	[16]

Although PTDs can facilitate the translocation of the desired molecules into cells, the exact mechanism is poorly understood. However, it is believed that basic residues and/or positive charge are crucial for PTDs' functions [14]. It has been hypothesized that penetratin and other basic amino acid-rich PTDs, like TAT interacts with and translocates through the lipid membrane by transient inverted - micelles formation [7]. In another proposed mechanism, TAT penetration is proven to require cell surface heparin sulphate proteoglycans (HSPGs) which are highly negative-charged and strongly hydrophilic. The proposed PTD-HSPG interaction seems to be consistent with the high arginine and lysine content of most PTDs, resulting in a positive charge at physiological pH. The positive residues likely interact with the negatively charged HSPG. Therefore it seems that the accessibility of these basic amino acid residues is important in order to achieve sufficient interaction with the HSPG [17].

Oxygen-dependent degradation domain (ODD)

Oxygen-dependent proteolysis is the primary means of regulating the transcription factor HIF-1α since it contains two highly conserved oxygen-dependent degradation residues (Pro-402 and Pro-564). After being hydroxylated in the presence of oxygen, the VHL E3 ubiquitin ligase interacts and targets HIF-1α for proteasomal degradation [18, 19]. Notably, among 2 residues being hydroxylated by VHL complex, Pro-564 has been proven to play a more crucial role in HIF-1α regulation in normoxia than Pro-402. Specifically, using hydroxylation-specific antibodies, Pro-564 was found to be hydroxylated prior to proline 402, and mutation of proline 564 results in a significant reduction in the hydroxylation of proline 402. Mutation of proline 402, however, has little effect on the hydroxylation of proline 564 [20]. In fact, a part of the HIF-1α ODD domain that contains Pro-564 residue has been reported to successfully guide the fused protein under the same oxygen-dependent regulation as HIF-1α [4, 21]. Furthermore, it has been reported that when mice are administered PTD fusion protein intraperitoneally (i.p.), the protein can be delivered into the tissues and cells of the entire body, including the brain [22]. Employment of HIF-derived domain ODD, thus, gives extensive applications for monitoring and targeting HIF-active cancers.

PTD-ODD fusion protein imaging probes specific to HIF-1-active cancers

Because HIF-1 activity is a hallmark for malignant tumors as well as ischemic diseases, bioprobes specific to HIF-1-active cells have been desired. Since PTD-ODD fusion proteins underlie the same ODD control as HIF-1α, they could serve as bioprobes

for imaging and treatment of the diseases related to HIF-1. In our lab, I first constructed PTD-ODD-β-gal or PTD-ODD-EGFP labelled with near-infrared fluorescent dye Cy5.5 and found that both the constructed probes showed high specificity for hypoxic HIF-active cells *in vitro* and *in vivo* [23]. After that, I constructed a recombinant protein PTD-ODD-HaloTag (POH) which contains an interchangeable labeling system. POH was labeled by covalent binding of near-infrared fluorescent (NIRF) dye-conjugated HaloTag-ligand to a specific site in the HaloTag domain so that the NIRF labeling would not affect the function of the PTD and ODD domains. I was able to monitor HIF-active regions after administration of near-infrared fluorescence-labeled POH (POH-N) to mouse cancer models. For the NIRF dyes, two NIRF dyes, IR800 (POH-I) and Alexa Fluor 750 (POH-A) was used and both of the bioprobes successfully delivered to subcutaneous or orthotopic HIF-active pancreatic cancer models. In contrast, these results cannot be achieved by the bioprobes bearing a point substitution mutation of Pro-564 (to Ala-564) in ODD domain and the bioprobes lacking PTD domain showed less amount and retention time in tumors. Thus, non-invasive fluorescent monitoring of HIF-active microenvironments in living animals using an oxygen-dependent degradation protein probe offers highly sensitive and specific detection of HIF-positive cells [12].

Treatment of HIF-active cancers by TAT-ODD-Procaspase-3

Together with the probes to monitor HIF-activities, I have constructed a fusion protein prodrug TAT-ODD-Procaspase-3 (TOP3) to target HIF-active cancer cells. TOP3 protein contains a TAT domain, which is derived from human immunodeficiency virus (HIV) and facilitates penetration of the protein through the mammalian phospholipid bilayer membranes. The second domain, the ODD, which is derived from HIF-1α, confers the hypoxia selective property of the fusion protein by causing the protein to be degraded in normoxic cells or remain stable in hypoxic cells. Under stressful conditions activated caspase-3 derived from the procaspase-3 domain will cause the hypoxic cells to undergo apoptosis (**Figure 3.1**).
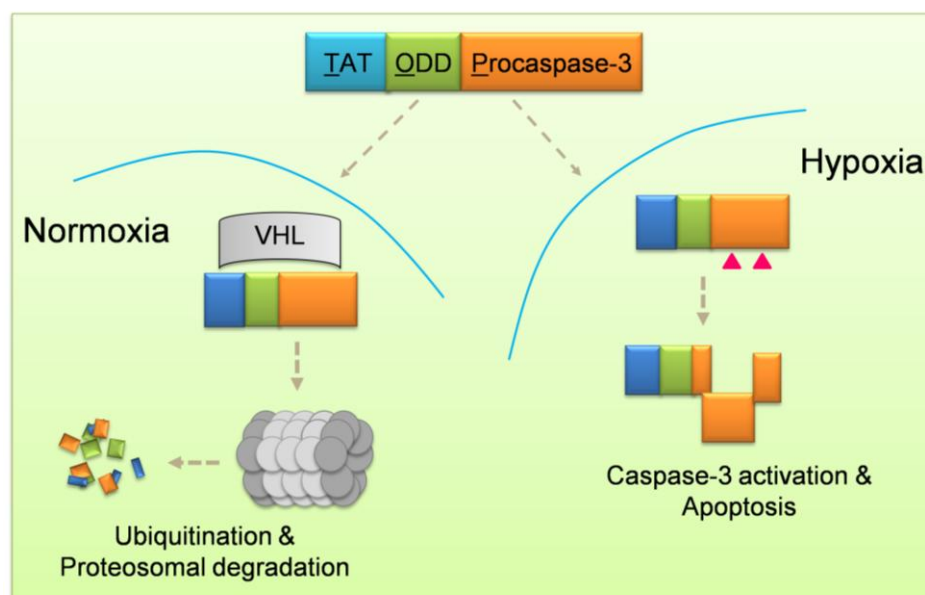
Figure 3.1. Mechanism of hypoxia-specific cytotoxicity of TOP3. TOP3 enters cells by the function of TAT domain and the ODD domain endows TOP3 with the same posttranslational regulation through ODD domain as HIF-1α. In hypoxic tumor cells, endogenous caspases are activated to some extent, Procaspase-3 is cleaved and the cells subsequently experienced apoptosis. When TOP3 enters normoxic cells, it is recognized by VHL and degraded through ubiquitin-proteasome system.

After constructing TOP3, we have confirmed the efficacy of the protein on several cell lines and mouse models. Procaspase-3 is a major executioner protein that is activated in several apoptotic pathways. Under hypoxic conditions, upstream caspase-3 is activated, inducing the cleavage of procaspase-3 followed by apoptosis of the cells. I previously reported the efficiency of TAT-ODD-Caspase-3 wild type (TAT-ODD-Casp3^{WT}) in reducing the size of tumors which was not achieved by TAT-ODD-mutant Caspase-3, suggesting specific stabilization and activation of the fusion protein in the hypoxic tumor cells [4]. Subsequently, TOP3 was proved to be effective in a malignant ascites model. Treatment with TOP3 impaired the growth of rat ascites MM1 cells in culture under hypoxic conditions by inducing apoptosis. Notably, intraperitoneal administration of TOP3 prolonged the life span of rats bearing a significant amount of malignant ascites, and 60% of the treated animals were cured without recurrence of ascites [24].

The protein drug TOP3 gained further achievements in selective killing HIF-active cancer cells in a subcutaneous model of the human cervical cancer cell line HeLa. In this

model, HIF-1 activity was monitored via an optical *in vivo* imaging system using a luciferase reporter gene under the regulation of a HIF-1-dependent promoter, 5HRE. Evaluation of the efficacy of a hypoxia-targeting prodrug, TOP3, using this optical imaging system revealed that hypoxic cells HeLa/5HRE-Luc were significantly diminished by TOP3. Also, immunohistochemical analysis of the TOP3-treated xenografts confirmed that hypoxic cells underwent apoptosis after TOP3 treatment [25].

The mechanism of TOP3 was further examined in cell culture model of a variety of cell lines including CFPAC-1 and MIA Paca-2 human pancreatic cancer cell lines, HeLa human cervical epithelial adenocarcinoma, A549 human lung adenocarcinoma, WiDr human colorectal adenocarcinoma and 786-O human renal carcinoma cell lines. Using these cell models, TOP3 was proved to be regulated similarly to HIF-1α. In a well-characterized osteolytic bone metastases model using MDA-MB-231 breast cancer cell line, HIF-1 and hypoxia were proven to contribute to the development of bone metastases. TOP3 selectively killed hypoxic MDA-MB-231 cells *in vitro* by its stabilization and activation of caspase-3-induced apoptosis. Furthermore, *in vivo* experiments showed that the i.p administration of TOP3 significantly reduced bone metastases as well as orthotopic tumors. These results support the notion that hypoxia makes a substantial contribution to the development of bone metastases of breast cancer and further confirm the efficiency of TOP3 [26].

POP33, a variant of TOP3, in which the TAT domain was replaced by a PTD domain was proven to give clear effects on suppression of peritoneal dissemination and extension the life span of treated mice in an orthotopic pancreatic cancer model [27]. Achievements in administration of TOP3 as well as POP33 for HIF-active cancers consolidate the important role of HIF-1 in malignant tumor and prove the requirements of HIF-1 targeting drug for hypoxic cancer treatment. The summary of cell lines and animal models on which the efficacy of TOP3 or POP33 have been evaluated is described in **Table 3.2**. Thus, in this study, I evaluated the efficacy of TOP3 when it was treated to pancreatic cancer cells SUIT-2, for the first time in our research progress. I hope that TOP3 can overcome the limitation of the chemotherapeutic drugs gemcitabine and TS-1 *in vitro*.

Table 3.2: Efficacy of TOP3 has been confirmed in several cell lines and mouse models. (-), only *in vitro* experiments were conducted.

Protein drug	Cell lines	Animal models	References
TOP3	Mouse fibroblast NIH/3T3	-	[4]
	Pancreatic cancer CFPAC-1	Subcutaneous	[4, 25, 28]
	Rat hepatoma MM1	Malignant ascites	[24]
	Cervical cancer HeLa	Subcutaneous	[21, 25, 28]
	Pancreatic cancer MIA PaCa-2	-	[21]
	Renal cell carcinoma 786-O	-	[21]
	Lung cancer A549	-	[21]
	Breast cancer MDA-MB-231	Orthotopic	[26]
POP33	Pancreatic cancer SUIT-2	Orthotopic	[27]

Materials and Methods

Expression and purification of TOP3

E. coli strain SoluBL21™ Competent (Genlantis, CA, USA) with protease deficiency was used to express GST-TOP3 protein. The GST-TOP3 expression plasmid-transformed _E. coli_ was pre-cultured in 500 ml of TB medium (1.2% peptone, 2.4% yeast extract, 72 mM K_2HPO4, 17 mM KH_2PO4 and 0.4% glycerol) at 200 rpm, $37^{o}C$ in bio-shaker BR-43FL (TAITEC, Saitama, Japan). When the optical density (OD) reached 1.8, 500 μL of 1M Isopropyl β-D-1-thiogalactopyranoside (IPTG) was added to the medium and the culture was continued with the conditions of 80 rpm, $20^{o}C$ overnight in bio-shaker BR-43FL (TAITEC, Saitama, Japan). When the OD reached around 8.0, the cells was collected by centrifugation at 8000 rpm, $4^{o}C$, 5 minutes by the refrigerated centrifuge MX305 (TOMY, Tokyo, Japan). The supernatant after centrifugation was discarded. The pellets of _E. coli_ cells were suspended in 120 mL of PBS (137 mM NaCl, 2.7 mM KCl, 8.0 mM $Na_2HPO_4.12H_2O$, 1.47 mM KH_2PO4). The suspension of _E. coli_ was frozen and thawed 3 times at $-80^{o}C$ freezer and $37^{o}C$ water bath, respectively. The suspension was subsequently sonicated several times on ice, 1 minute each time by ultrasonic homogenizer UD201 (TOMY). The sonicated suspension was added with 10% Triton X-100 to get the final concentration of 1% and kept on ice for 1 hour.

The suspension was then centrifuged at 91,000 × g, $4^{o}C$, 30 minutes. The supernatant with the target protein was added to 0.6 g pre-washed reduced glutathione agarose (Sigma-Aldrich, St. Louis, MO, USA) and mildly rotated over night by a rotator at $4^{o}C$.

The GST-TOP3-Glutathione agarose complex was wash 3 times by 10-time volume of pre-cooled PreScission protease cleavage buffer (50 mM Tris pH 7.0, 150 mM NaCl, 1 mM EDTA) by centrifugation at1,000 × g, $4^{o}C$, 5 minutes. After washing, 400 μL of PreScission protease cleavage buffer, 5 μL of PreScission protease (GE Healthcare, Little Chalfont, UK) were added to each mL of GST-TOP3-Glutathione agarose and the reaction was carried out for 2 days by a rotator at $4^{o}C$.

The supernatant after the reaction was collected by centrifugation at 1500 × g, $4^{o}C$, 5 minutes and the buffer was exchanged to 10 mM Tris-HCl pH 8.0 by dialysis overnight using Snakeskin Dialysis Tubing 10K MWCO (Thermo Fisher Scientific, Waltham, MA,

USA). The final protein solution then was concentrated by ficoll (Nacalai Tesque, Kyoto, Japan) and kept at -80$^{\mathrm{o}}$C for subsequent experiments.

BCA assay

In BCA assay (Thermo Fisher Scientific), bovine serum albumin in the kit was prepared at a serial dilution to the final concentration of 0, 25, 125, 250, 500, and 1000 µg/mL. The working reagent was made by mixing solution A: solution B at 50:1 ratio. 25 µL of the sample was mixed with 200 µL of working solution in each well of a 96-well plate and the measurement was taken place by micro plate reader Model 680XR (Bio-Rad, Tokyo, Japan) at 595 nm after developing the signal in 30 minutes and shaking in 10 seconds. A standard curve was made with the correlation between the absorbance values and the concentration of the proteins in the serial dilution. The concentration of TOP3 was calculated via this standard curve based on its absorbance.

SDS-PAGE analysis

TOP3 was mixed with equal volume of $2 \times$ sample buffer (125 mM Tris-HCl pH 6.8, 4% SDS, 20% glycerol, 10% β-mercaptoethanol, 0.01% bromophenol blue). The samples were then heated at 95$^{\mathrm{o}}$C, centrifuge at 10,000 x g, room temperature and vortex with 5 minutes in each step. 20 µL of prepared samples was applied to 12.5% SDS-PAGE gel and the gel was run at 200 mA, 150V, 90 minutes (constant voltage). The gel was then stained with Coomassie Brilliant Blue R-250 (CBB) solution (0.15% CBB, 12.5% acetic acid) for 4 hours and destained by water until the bands of protein were clear. The relative purity of the protein was subsequently relatively calculated by Image J software.

Cell culture and TOP treatment *in vitro*

SUIT-2 human pancreatic cancer cells were purchased from the Japanese Cancer Research Resource Bank (Osaka, Japan) and established SUIT-2/HRE-Luc cells [27] were maintain in DMEM (Life Technologies, Carlsbad, CA, USA) supplemented with 5% FBS, penicillin (100 units /mL) and streptomycin (100 µg /mL) (Nacalai Tesque) in a multigas incubator (Sanyo, Osaka, Japan). For the hypoxic experimental setup, a hypoxic chamber (Ruskinn, South Wales, UK) or a hypoxic incubator (Astec, Fukuoka, Japan) was used to attain an oxygen level of 0.1% or 1%, respectively.

Flow cytometry analysis of apoptotic cells

Cells were seeded at 1.5×10^5 cells/well in 6-well plates and precultured in normoxia overnight. For the samples in hypoxia, the medium was replaced with fresh medium containing 0.2% FBS and 500 mg/L glucose, and gemcitabine (15 nM) or 5-FU (50 µM) were added on the following day. The plates were then incubated in the hypoxic incubator at 1% O_2 for 30 hours before addition of TOP3 (20 µg/mL) and further incubation under the same conditions for 18 hours. Cells were prepared with hypotonic fluorochrome solution (50 µg/mL PI in 0.1% sodium citrate-0.1% Triton X-100) and analyzed by EC800 Analyzer (Sony, Tokyo, Japan). For samples in severe hypoxia, the culture medium was DMEM supplemented with 0.1% FBS and 100mg/L glucose under 0.1% oxygen in the hypoxic chamber and cells were treated with the same doses of gemcitabine, 5-FU, and TOP3.

Results

Expression and purification of TOP3 protein

Our strategy to get TOP3 for *in vitro* and *in vivo* experiment is overexpression of Glutathione S transferase (GST)-tagged TOP3 in *E. coli* and subsequently purified the tagged-protein by reduced glutathione agarose beads. The GST-TOP3 then was cleaved the tag by PreScission protease. During the purification process, small aliquots of samples were collected to monitor the relevancy of each step. I confirmed the existence of purified protein TOP3 at the expected size with a purity of around 70% (**Figure 3.2**).
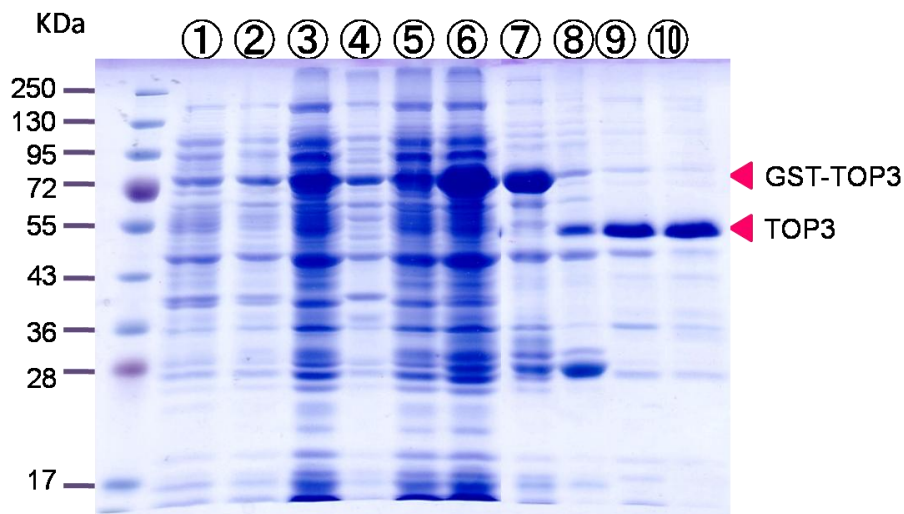

Figure 3.2. Representative SDS-PAGE analysis in purification process of TOP3

① E. *coli* culture before induction by IPTG, A600=1.8

② *E. coli* culture after induction by 1 mM IPTG, A600=5.6

③ *E.coli* lysate after sonication, supernatant

④ *E.coli* lysate after sonication, pellet

⑤ Supernatant after binding to GST beads

⑥ GST beads after binding with TOP3

⑦ GST beads after wash 3 times by PreScission cleavage buffer

⑧ GST beads after cleavage

⑨ TOP3 fraction after cleavage

⑩ TOP3 after dialysis

Antitumor effects of TOP3 *in vitro*

Because of the resistance of SUIT-2 to gemcitabine and TS-1 in hypoxia (1% O_2) and severe hypoxia (0.1% O_2), respectively, I expected that combination treatments of TOP3 with gemcitabine or TS-1 would more efficiently decrease the viability of both normoxic and hypoxic cancer cells. To mimic *in vivo* conditions in tumor hypoxia, SUIT-2 cells were cultured in medium containing low FBS and low glucose (starved medium) in hypoxia (1% O_2). SUIT-2 is highly adapted to hypoxia and its viability was not significantly influenced by hypoxic treatment alone (**Figure 3.3a**). However, SUIT-2 cells cultured in the starved medium under hypoxic (1% O_2) and severe hypoxic (0.1% O_2) conditions showed a significantly increased susceptibility to TOP3 compared with cells under normoxic conditions (**Figure 3.3b, c**), suggesting that the starvation conditions increased stress responses in the cells leading to activation of caspases and eventually to TOP3 activation. TOP3 treatment alone under starvation and hypoxic conditions successfully induced apoptotic cell death as indicated by a significant increase in the sub-G1 fraction in flow cytometry analysis. Under the same conditions, treatment with gemcitabine or 5-FU in combination with TOP3 did not increase cell death (**Figure 3.3b, c**). Notably, the effects of TOP3 with gemcitabine or 5-FU were not observed in parallel samples under normoxic conditions. These results clearly demonstrate that TOP3 targets distinct cells from gemcitabine and 5-FU.
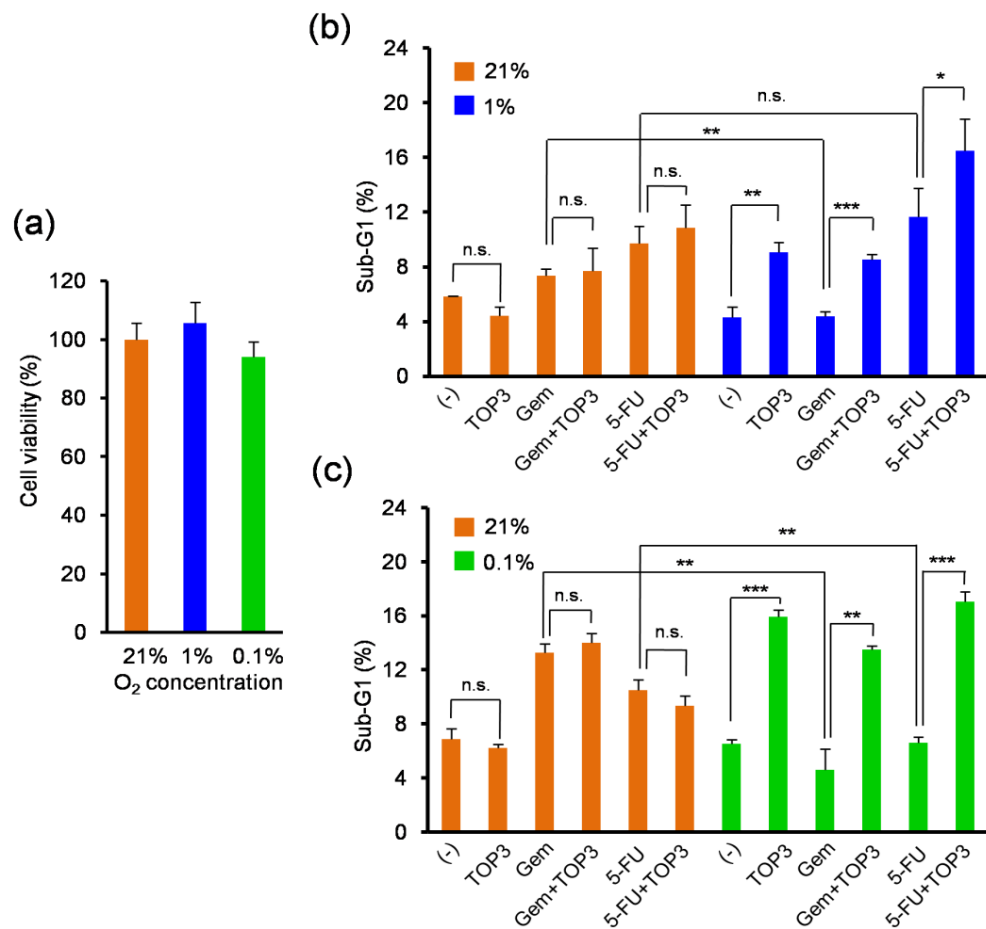
Figure 3.3. Effects of drugs on pancreatic cancer cells under conditions of oxygen and nutrient shortage. (**a**) Viability of SUIT-2 cells after hypoxic (0.1% and 1% O_2) treatment for 72 hours determined by WST-1 assay. The OD obtained from hypoxia-treated SUIT-2 cells was normalized to the OD of SUIT-2 cells cultured under normoxic conditions and is shown as cell viability (%). (**b**, **c**) SUIT-2 cells were cultured under starved and hypoxic (1% O_2, 0.2% FBS with 500 mg/L glucose) conditions (**b**) or severe hypoxic and starved (0.1% O_2, 0.1% FBS, 100 mg/L glucose) conditions (**c**) with or without gemcitabine (15 nM) or 5-FU (50 μM) for 30 hours. TOP3 (20 μg/mL) was added and the cells were further incubated for 18 hours under the same conditions. The DNA content was analyzed by FACS and the sub-G1 fraction (%) is indicated in the figure. n = 4. The experiments were repeated three times and representative data are shown.

Discussion

Cytotoxicity effect of TOP3 on hypoxic cells is acquired by processing of procaspase-3 domain to active caspase-3 and the subsequent trigger of cellular apoptosis via intrinsic pathway. This mechanism only occurs in HIF-active cells in tumors because TOP3 is degraded in HIF-negative cells through the VHL-mediated destruction. In this research, I confirmed the limited efficacy of gemcitabine and TS-1 in pancreatic cancers with tumor hypoxia by *in vitro* data obtained under conditions that mimic tumor hypoxia. Under hypoxic and severe hypoxic conditions with starved medium, the cytotoxic effects of gemcitabine were totally abolished. On the other hand, the effects of 5-FU were only affected by severe hypoxic treatment with starved medium (**Figure 3.3**), which was correlated with experiment data in **Figure 2.7**. Overall, under starved and severe hypoxic conditions, the resistance of SUIT-2 to the drugs was more remarkable; gemcitabine and 5-FU had no influence on percentage of cell death and only TOP3 effects were observed under these conditions (**Figure 3.3b, c**).

In this experiment, I used TOP3 with a purity of about 70% for the experiments. Even so, I could observe the specificity of activation of TOP3 *in vitro* by the increase of sub-G1 cells, which was not observed under normoxic conditions. Thus, it is expected that TOP3 with higher purity may further induce cell death to hypoxic cells. Therefore, additional purification methods together with optimization of current protocol are necessary to improve the purity of TOP3 for subsequent studies.

References

1. Beerens, A.M., et al., *Protein transduction domains and their utility in gene therapy.* Curr Gene Ther, 2003. **3**(5): p. 486-94.

2. Wender, P.A., et al., *The design, synthesis, and evaluation of molecules that enable or enhance cellular uptake: peptoid molecular transporters.* Proc Natl Acad Sci U S A, 2000. **97**(24): p. 13003-8.

3. Zhou, G., et al., *Neuroprotective effect of TAT PTD-Ngb fusion protein on primary cortical neurons against hypoxia-induced apoptosis.* Neurol Sci, 2013.

4. Harada, H., M. Hiraoka, and S. Kizaka-Kondoh, *Antitumor effect of TAT-oxygen-dependent degradation-caspase-3 fusion protein specifically stabilized and activated in hypoxic tumor cells.* Cancer Res, 2002. **62**(7): p. 2013-8.

5. Elliott, G. and P. O'Hare, *Intercellular trafficking and protein delivery by a herpesvirus structural protein.* Cell, 1997. **88**(2): p. 223-33.

6. Bennett, R.P., B. Dalby, and P.M. Guy, *Protein delivery using VP22.* Nat Biotechnol, 2002. **20**(1): p. 20.

7. Derossi, D., et al., *Cell internalization of the third helix of the Antennapedia homeodomain is receptor-independent.* J Biol Chem, 1996. **271**(30): p. 18188-93.

8. Han, K., et al., *Efficient intracellular delivery of GFP by homeodomains of Drosophila Fushi-tarazu and Engrailed proteins.* Mol Cells, 2000. **10**(6): p. 728-32.

9. Chatelin, L., et al., *Transcription factor hoxa-5 is taken up by cells in culture and conveyed to their nuclei.* Mech Dev, 1996. **55**(2): p. 111-7.

10. Ippel, H., et al., *The solution structure of the homeodomain of the rat insulin-gene enhancer protein isl-1. Comparison with other homeodomains.* J Mol Biol, 1999. **288**(4): p. 689-703.

11. Karlsson, O., et al., *Insulin gene enhancer binding protein Isl-1 is a member of a novel class of proteins containing both a homeo- and a Cys-His domain.* Nature, 1990. **344**(6269): p. 879-82.

12. Kuchimaru, T., et al., *In vivo imaging of HIF-active tumors by an oxygen-dependent degradation protein probe with an interchangeable labeling system.* PLoS One, 2010. **5**(12): p. e15736.

13. Ho, A., et al., *Synthetic protein transduction domains: enhanced transduction potential in vitro and in vivo.* Cancer Res, 2001. **61**(2): p. 474-7.

14. Mi, Z., et al., *Characterization of a class of cationic peptides able to facilitate efficient protein transduction in vitro and in vivo.* Mol Ther, 2000. **2**(4): p. 339-47.

15. Pooga, M., et al., *Cell penetration by transportan.* FASEB J, 1998. **12**(1): p. 67-77.

16.   Garcia-Echeverria, C., et al., *A new Antennapedia-derived vector for intracellular delivery of exogenous compounds.* Bioorg Med Chem Lett, 2001. **11**(11): p. 1363-6.

17.   Tyagi, M., et al., *Internalization of HIV-1 tat requires cell surface heparan sulfate proteoglycans.* J Biol Chem, 2001. **276**(5): p. 3254-61.

18.   Kizaka-Kondoh, S., et al., *The HIF-1-active microenvironment: an environmental target for cancer therapy.* Adv Drug Deliv Rev, 2009. **61**(7-8): p. 623-32.

19.   Semenza, G.L., *Targeting HIF-1 for cancer therapy.* Nat Rev Cancer, 2003. **3**(10): p. 721-32.

20.   Chan, D.A., et al., *Coordinate regulation of the oxygen-dependent degradation domains of hypoxia-inducible factor 1 alpha.* Mol Cell Biol, 2005. **25**(15): p. 6415-26.

21.   Harada, H., S. Kizaka-Kondoh, and M. Hiraoka, *Mechanism of hypoxia-specific cytotoxicity of procaspase-3 fused with a VHL-mediated protein destruction motif of HIF-1alpha containing Pro564.* FEBS Lett, 2006. **580**(24): p. 5718-22.

22.   Schwarze, S.R., et al., *In vivo protein transduction: delivery of a biologically active protein into the mouse.* Science, 1999. **285**(5433): p. 1569-72.

23.   Kizaka-Kondoh, S., S. Tanaka, and M. Hiraoka, *Imaging and Targeting of the Hypoxia-inducible Factor 1-active Microenvironment.* J Toxicol Pathol, 2009. **22**(2): p. 93-100.

24.   Inoue, M., et al., *Targeting hypoxic cancer cells with a protein prodrug is effective in experimental malignant ascites.* Int J Oncol, 2004. **25**(3): p. 713-20.

25.   Harada, H., S. Kizaka-Kondoh, and M. Hiraoka, *Optical imaging of tumor hypoxia and evaluation of efficacy of a hypoxia-targeting drug in living animals.* Mol Imaging, 2005. **4**(3): p. 182-93.

26.   Hiraga, T., et al., *Hypoxia and hypoxia-inducible factor-1 expression enhance osteolytic bone metastases of breast cancer.* Cancer Res, 2007. **67**(9): p. 4157-63.

27.   Kizaka-Kondoh, S., et al., *Selective killing of hypoxia-inducible factor-1-active cells improves survival in a mouse model of invasive and metastatic pancreatic cancer.* Clin Cancer Res, 2009. **15**(10): p. 3433-41.

28.   Harada, H., et al., *Significance of HIF-1-active cells in angiogenesis and radioresistance.* Oncogene, 2007. **26**(54): p. 7508-16.

Chapter 4

Evaluation of the efficacy of TOP3 *in vivo* in combination with gemcitabine and TS-1

Abstract

In previous chapters, I confirmed that gemcitabine/TS-1 and TOP3 target different cell populations. Therefore, it was expected that treatment of pancreatic cancer, which often contains heterogenous microenvironment with various oxygen and nutrition levels, by combination of chemotherapeutic drugs gemcitabine/TS-1 with TOP3 overcame the limitation of each drug and improved treatment outcomes. In order to examine the above hypothesis, I used orthotopic pancreatic cancer mouse model with SUIT-2/HRE-Luc cells, which generate bioluminescent signal in response to HIF activity. I confirmed that the bioluminescent signals of SUIT-2 cells were highly correlated with the expression levels of HIFs *in vitro* when the cells were exposed to hypoxic conditions. After being transplanted into the pancreas of immunodeficient mice, SUIT-2/HRE-Luc cells were well colonized and steadily progressed in non-treated control mice. On the other hand, the mice received single treatments of TOP3, gemcitabine or TS-1 showed a delay in the progression of the HIF-active signals, which proved the efficacy of each drugs. Strikingly, the combination of TOP3 with gemcitabine or TS-1 further enhanced the treatment outcomes achieved by each drug. In survival analysis, I also observed the consistent results with the suppression of the bioluminescent signals: single treatment prolonged the survival of the treated mice and all the combination treatments further improved survival rates.

Introduction

Tumor microenvironment of hypoxic cancers has been reported to contain both normoxic and desmoplastic regions [1], which often proved to be hypoxic [2]. Currently, single treatment of this devastating cancer by normoxia targeting drugs only provided limited benefits to the patients. Specifically, only 25-30% of pancreatic patients show response to the standard drugs gemcitabine and TS-1 [3]. Thus, several research groups have been extensively focussing on developing drugs targeting hypoxic regions of these heterogeneous cancers. These drugs are designs based on five different chemical moieties including nitro groups, quinones, aromatic *N*-oxides, aliphatic *N*-oxides and transition metals which are able to be activated under reduced environment of tumor hypoxia, thus trigger the cytotoxic effect within hypoxic regions. The summary of most advanced prodrugs to treat hypoxic cancers is shown in **Table 4.1**.

Table 4.1: Several hypoxia-activated prodrugs are under developed worldwide for the treatment of hypoxic cancers. Most of them are currently progressing in clinical trial phases.

Drugs	Current status	Chemical moieties	References
Tirapazamine	Phase III	Aromatic *N*-oxide	[4]
Apaziquone	Phase III	Quinone	[5]
TH-302	Phase II	Nitro	[6]
PR-104	Phase II	Nitro	[7]
Banoxantrone (AQ4N)	Phase II	Aliphatic *N*-oxide	[8]
RH1	Phase I	Quinone	[9]
NLCQ-1	Preclinical	Nitro	[10]

In addition, it is expected that combination treatment of the drugs which target different cancer cell populations of hypoxic cancers will further enhance the efficacy achieved by each drug for treatment of this severe cancer. However, though the above hypoxia-activated prodrugs were effective in killing hypoxic cells to some extent, their combination with radiotherapy or chemotherapy rarely yielded positive outcomes [11-13]. These drugs may cause severe off-target toxicity and are therefore not recommended for long-term treatment [14]. On the other hand, it has been proved that more significant efficacy of TOP3 is exhibited in killing tumor cells in long-term schedules of combination of TOP3 with radiation therapy compared to separate treatments. Most notably, there was a noteworthy decrease in microvessel density within tumors was recorded. Eradication of

HIF-1-active hypoxic cells in the xenografts during irradiation exhibited remarkable suppression in angiogenesis and strong enhancement in a long-term growth suppression of tumor xenografts. This indicates that the combination treatment enhanced tumor suppression by anti-angiogenesis activity [15].

However, the efficacy of TOP3 in combination with chemotherapeutic drugs has not been evaluated *in vivo*. In this chapter, I reported the combination of TOP3 with chemotherapeutic drugs gemcitabine/TS-1 for the first time. I hope that the combination treatment will overcome the limitation of each drug in suppressing cancer cells and further prolonged the survival of the xenografts.

Materials and Methods

Luciferase assay

In order to screen for SUIT-2/HRE-Luc cell clones which highly express luciferase activity under hypoxic conditions, the cells were seeded at 5×10^4 cells in a 24-well plate, and pre-cultured in normoxia for 12 hours. The cells were further incubated in hypoxic incubator at 37°C, 1% O_2, 5% CO_2 for 24 hours and trypsinized by 100 μL of 0.25 w/v % Trypsin-EDTA (0.25%) (Thermo Fisher Scientific) and collected into eppendorf tubes. The cells then were collected by centrifugation at $10,000 \times$ g, 4°C, 3 minutes. The supernatants were removed and the cell pellets were lysed by 10 μL Passive Lysis Buffer (PLB) (Promega, Madison, WI, USA). The firely luciferase activity was measured after the addition of 20 μL luciferase assay reagent (Promega) using the Modolus luminometer (Turner Biosystems, Sunnyvale, CA, USA).

For measuring luciferase activity of SUIT-2/HRE-Luc cell line induced under hypoxic conditions overtime, the cells were seeded at 5×10^4 cells in 24-well plates, and then pre-cultured in normoxia for 12 hours. Subsequently, the cells were further incubated in the hypoxic incubator at 37°C, 1% O_2, 5% CO_2 for 0, 3, 6, 12, 24 and 36 hours. The cell lysate after directly being lysed by 100 μL PLB was then centrifuged at $10,000 \times$ g, 4°C, 3 minutes and the luciferase activity was measured using 10 μL of the supernatant with 20 μL luciferase assay reagent.

Dual luciferase assay

pEF/HRE-RLuc plasmid was constructed by substituting the coding sequence of firefly luciferase (Fluc) in pEF/HRE-FLuc [16]. The coding sequence of Renilla luciferase (Rluc) was amplified from pRluc [pRL-CMV] (Promega). VHL-786-O cells (5×10^4 cells/well) were seeded in a 24-well plate. After overnight incubation, pEF/HRE-RLuc was co-transfected with pEF-FLuc using X-treamGENE reagent (Roche Diagnostics, Indianapolis, IN, USA) according to the manufacturer's instructions. The cells were further incubated in 21% or 1% O_2 for 16 hours and harvested for analysis using the Dual-luciferase Reporter Assay system (Promega). Bioluminescence signals of RLuc were divided by those of FLuc to normalize the signal.

Western blotting

SUIT-2 cells were seeded at 1×10^5 cells on 6-well plates, pre-incubated for 12 hours in normoxia and further cultured in hypoxia at 37°C, 1% O_2, 5% CO_2 for 24 hours. The cell lysate was collected after directly added with 200 μL 2 × sample buffer. The samples were then heated at 95°C, centrifuged at room temperature at $10,000 \times g$, and vortexed for 5 minutes in each step. 20 μL of prepared samples was applied to 10% SDS-PAGE gel and run at 200 mA, 150V, 90 minutes (constant voltage). For Western blot to detect HIFs protein of SUIT-2/HRE-Luc in time course, cells were incubated in hypoxia at at 37°C, 1% O_2, 5% CO_2 for 0, 3, 6, 12, 24 and 36 h.

Discontinuous buffers (I: 80% 375 mM Tris-HCl pH 10.4 + 10% methanol, II: 80% 25 mM Tris-HCl pH 10.4 + 10% methanol, III: 80% 25 mM Tris-HCl pH 9.4, 40 mM 6-amino hexa acid + 10% methanol) was used for transferring the proteins from the SDS-PAGE gel to nitrocellulose membranes by the settings of 200 mA, 20V, 60 minutes (constant voltage). The membrane then was washed by TBST 5 minutes for 3 times, and blocked with 5% skim milk in TBST for 1 hour at room temperature. The binding of primary antibody and secondary antibody to the membrane were carried on overnight at 4^0C and 1 hour at room temperature, respectively. The membrane was washed by TBST 5 minutes for 3 times and detected by LAS 4000 (Fujifilm, Tokyo, Japan) after adding ECL Prime Western Blotting Detecting reagent (GE Healthcare, Little Chalfont, UK). Before and after the addition of primary and secondary antibody, the membrane was washed by TBST 5 minutes for 3 times. All the used antibodies are diluted at 1/1000 ratio and they are listed in **Table 4.2**.

Table 4.2: Antibodies used in Western blot experiments.

	Antibody name	Company	Product code
1st antibody	Anti-Actin mouse monoclonal Ab	Sigma-Aldrich	A4700
	Anti-HIF-1α rabbit polyclonal Ab	Novus Biologicals	A NB100-149
	Anti-HIF-2α rabbit polyclonal Ab	Novus Biologicals	NB100-149
2nd antibody	Anti-mouse IgG HRP-linked Ab	Cell Signaling Technology	#7076
	Anti-rabbit IgG HRP-linked Ab	Cell Signaling Technology	#7074

Animal experiments

BALB/c nu/nu male mice 5 week-old were purchased from Oriental Yeast Co. Ltd. and the *in vivo* experiment was started when the mice were 6-week old. All the animal experiments were performed with the approval of the Animal Experiment Committees of Tokyo Institute of Technology and conducted according to relevant national and international guidelines.

Orthotopic transplantation

SUIT-2/HRE-Luc cells were collected at the concentration of 1×10^5 cells/10 μL PBS and mixed with an equal volume of Geltrex (Life Technologies, Carlsbad, CA, USA). Generally, mice were anesthetized by the 10-time dilution of Somnopentyl anesthetic reagent (MSD Animal Health, Tokyo, Japan) with saline (Otsuka Pharmaceutical, Tokyo, Japan) according to their body weight and a small incision in the abdomen was made. By using cotton swab, the pancreas was externalized right under the liver. The total volume of 20 μL was then injected directly into the exposed pancreas by a 1 mL syringe needle gauge 27. After transplantation, the pancreas was returned back to the former position. The incision was closed by wound clips and sterilized by Isojin antiseptic solution (Meiji Seika Pharma, Tokyo, Japan).

In vivo imaging

Mice were anesthetized by Escain inhalation anesthetic solution (Mylan Pharmaceuticals, Canonsburg, PA, USA) and i.p injected with 200 μL D-Luciferin (10 mg/mL in PBS, Promega). The bioluminescent signals were recorded using IVIS spectrum (Perkin Elmer, Waltham, MA, USA) 15 minutes after the D-Luciferin injection with the exposure time of 1 minute.

Preparation and administration of TOP3, gemcitabine and TS-1

When the photon counts were approximately 1×10^5 photons/s for each region of interest, the mice were randomly divided into control and treatment groups for experiments and the treatments were started. TOP3 was i.p. injected into tumor-bearing mice at a dose of 10 mg/kg at 3- or 4-day intervals. TS-1 was dissolved in 0.5 % (w/v) hydroxypropyl methylcellulose (Shin-Etsu Chemical, Tokyo, Japan) and the mice were treated with 10 mg/kg TS-1 for 5 consecutive days per week by oral gavage. Gemcitabine was dissolved in PBS and i.p. administered to the mice at a dose of 50 mg/kg every 3 days. For combination treatments, the dosage and treatment schedule of single and combination treatments are

indicated in **Table 4.3**. The concentration of TS-1 throughout the experiment was calculated based on the concentration of the active component 5-FU.

Table 4.3: Treatment schedule for the animal experiments in which TOP3 was combined with gemcitabine (Gem) and TS-1

Groups	n	Drugs	Dose (mg/kg)	Schedule
Control	9	-	-	-
TOP3	8	TOP3	10	Every 3 days, i.p.
Gem	8	Gem	50	Every 3 days, i.p.
TOP3+Gem	8	TOP3	10	Every 3 days, i.p., start at day +1
		Gem	10	Every 3 days, i.p., start at day 0
Control	8	-	-	-
TOP3	7	TOP3	10	Every 4 days, i.p.
TS-1	8	TS-1	10	5 consecutive days/week. p.o.
TOP3+TS-1	8	TOP3	10	Every 4 days, i.p.
		TS-1	10	5 consecutive days/week, p.o.
n: number of treated mice; i.p.: intraperitoneal injection, p.o.; oral administration				

Statistical analysis

Data are represented as mean ± SEM (standard error of the mean) and significant differences were calculated by unpaired Student's *t*-test unless otherwise indicated. For *in vivo* experimental data, analysis of variance was used to analyze differences between group means. Overall significant difference among group means was analyzed using Tukey's honest significant difference. For survival analysis, the Kaplan–Meier method was used to determine survival curves, and comparisons between the curves were performed by log-rank test in R analysis. For each comparison, *P*-values < 0.05 were considered statistically significant.

Results

Establishment of SUIT-2 cell line with HIF-responsive reporter

In order to monitor the progression of HIF-active tumors *in vivo*, I established SUIT-2/HRE-Luc cell line which generates bioluminescent signal specifically only in HIF-active cells. A reporter plasmid containing *Fluc* gene downstream of CMV promoter and 5 tandem repeats of the HIF binding sequence, hypoxia responsive element (HRE), was transfected into wild type SUIT-2 cells. This HRE sequence is derived from human VEGF gene with the sequence of AACAGGTCCTCTT. The transfected cell line was then selected and stably maintained in medium containing 1mg/ mL G418 antibiotic (Life Technologies). The schematic of the luciferase reporter gene is depicted in **Figure 4.1.**
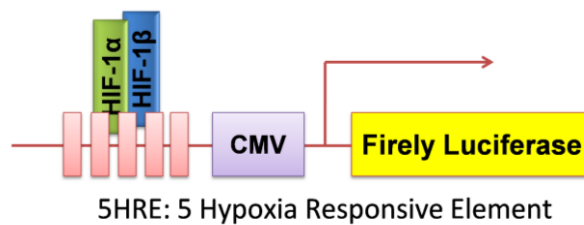
Figure 4.1. The structure of HIF-reponsive reporter in SUIT-2/HRE-Luc

Under hypoxic conditions (1% O_2) SUIT-2/HRE-luc expressed luciferase activity significantly higher than under normoxic conditions. SUIT-2/HRE-Luc cells expressed both HIF-1α and HIF-2α proteins and the intensity of bioluminescence produced by the cells correlated well with expression levels of these proteins. Specifically, both the HIF proteins and luciferase activity increased about 6 hours after hypoxia treatment, suggesting the time lag necessary for binding of HIF proteins to the 5HRE sequence of the reporter and induction of luciferase expression afterwards (**Figure 4.2a, b**). Because HIF-1 and HIF-2 bind to the same HRE sequence, HIF-2 may also be able to bind to the 5HRE because VEGF expression was reported to be regulated by HIF-2 as well as HIF-1. I examined the response of the HRE-Luc reporter gene in 786-O, a renal cell carcinoma cell line that harbors a mutation in the VHL gene and expresses only HIF-2α. HRE-luciferase expression in 786-O-VHL cells, in which a functional VHL gene has been introduced, was significantly increased by hypoxic treatment (**Figure 4.2c**), indicating that HIF-2 also functions as transcription factor for the 5HRE promoter. Therefore, an *in vivo* model using this cell line can be used to monitor both HIF-1 and HIF-2 activities. These results strongly

indicate the efficacy of the constructed reporter for HIF-activity and the validity of using the established cell line for subsequent experiments.
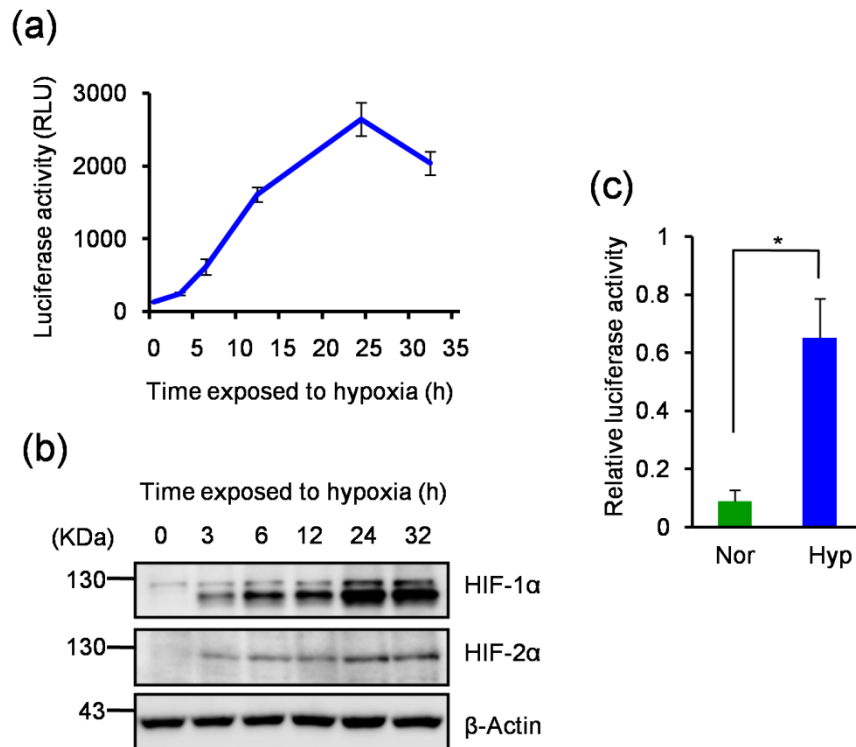

Figure 4.2. The HRE-Luc reporter system is suitable for evaluation of HIF activity. (**a**, **b**) SUIT-2/HRE-Luc cells cultured under normoxic conditions were exposed to hypoxic conditions (1% O_2) for the indicated time periods and luciferase activity (a) and HIFα protein levels (**b**) were analyzed. The bioluminescent intensity of luciferase is shown as relative light units (RLU). n=3. (**c**) 786-O-VHL cells were established by introducing wild-type VHL expression vector into VHL-null 786-O cells. 786-O-VHL cells were co-transfected with HRE-RLuc and pEF-FLuc reporter plasmids and cultured under normoxic or hypoxic (1% O_2) conditions. The bioluminescent intensity of RLuc was divided by that of Fluc and the normalized signal is shown as relative luciferase activity.

In vivo imaging of the progression of hypoxic cancer cells in the xenografts

I transplanted SUIT/HRE-Luc cells to the pancreas of the mice and measured the intensity of the bioluminescent signal specified as photons/second/region of interest. The bioluminescent signals from SUIT2/HRE-Luc xenografts reflect HIF activity in the cells. From previous experiments in our lab, I observed the peaks of the photon counpts between

13-15 minutes after D-Luciferin injection. Therefore, in this experiment, I acquired images of the xenografts 15 minutes after injection.

In my model, after transplantation of 1×10^5 cells into the pancreas, around 1 week afterwards I can detect the clear signal over background of the hypoxic cells in the abdomen cavity relatively to the pancreas location. The hypoxic cells developed signal locally in the pancreas within the first week. However, in the second week, the signal tended to spread in the abdomen which significantly led to the enhancement of the signal in the next 1 or 2 weeks. Without any treatments, the mice experienced severe accumulation of ascetic fluid throughout the abdomen and died approximately more than one month after transplantation. The progression of the hypoxic cells was clearly visualized by the *in vivo* imaging system and is depicted in **Figure 4.3**.
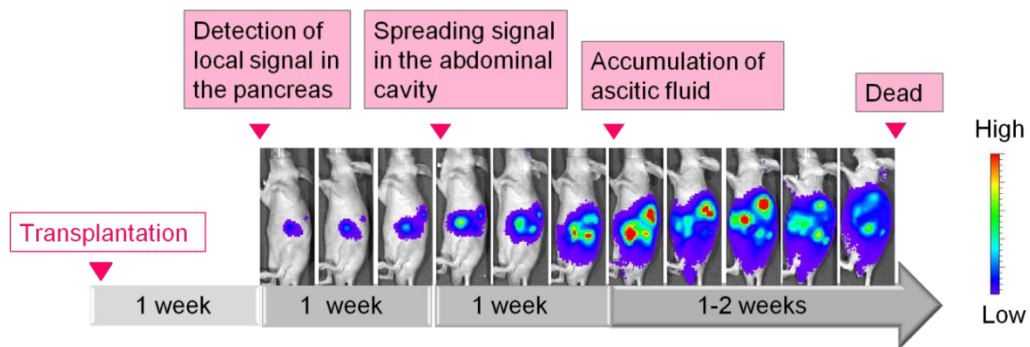
Figure 4.3: Representative images of HIF-1 activity in an orthotopic model of pancreatic cancer. Approximately 4-5 weeks after transplantation, the mice died with severe accumulation of ascitic fluid in the abdomen.

Enhanced antitumor effects of gemcitabine and TS-1 by combination treatment with TOP3

Motivated by the *in vitro* results, I next assessed the therapeutic effects of the combination treatments in an orthotopic pancreatic cancer model using SUIT-2/HRE-Luc cells [17], in which the luciferase activity was highly correlated with HIFα expression (**Figure 4.2**) and thus correlated with HIF activity [18]. Using this model, I was able to monitor the progression of HIF-active cancer cells in real-time by *in vivo* bioluminescence imaging of SUIT-2/HRE-Luc xenografts. I monitored the bioluminescence every 4 days throughout the experiment (**Figure 4.4a, b**). The drug dosages and schedule of the combination treatments are summarized in **Table 4.3**. HIF activity in the xenografts of untreated mice increased rapidly and the mice eventually died with accumulation of ascites and peritoneal

dissemination within 4 weeks after the initial detection of significant HIF-active signals. In contrast, mice treated with TOP3 exhibited bioluminescence signals that were localized in the pancreas for longer periods, indicating effective killing of HIF-active cancer cells in the pancreas. Strikingly, the bioluminescence signals in the mice treated with gemcitabine or TS-1 were also localized in the pancreas for periods compatible with the signals in the TOP3-treated mice. As expected, the combination treatment further extended the duration of the localized signal in the pancreas. The bioluminescence signals of gemcitabine- and TS-1-treated groups were analyzed on days 20 and 16 respectively because these were the last days that all mice in each control group were alive (**Figure 4.4c, d**). The summary of significant values of **Figure 4.4c, d** is indicated in **Table 4.4**. The results clearly demonstrated that TOP3 enhanced the efficacy of gemcitabine and TS-1 against pancreatic cancer in combination treatments.
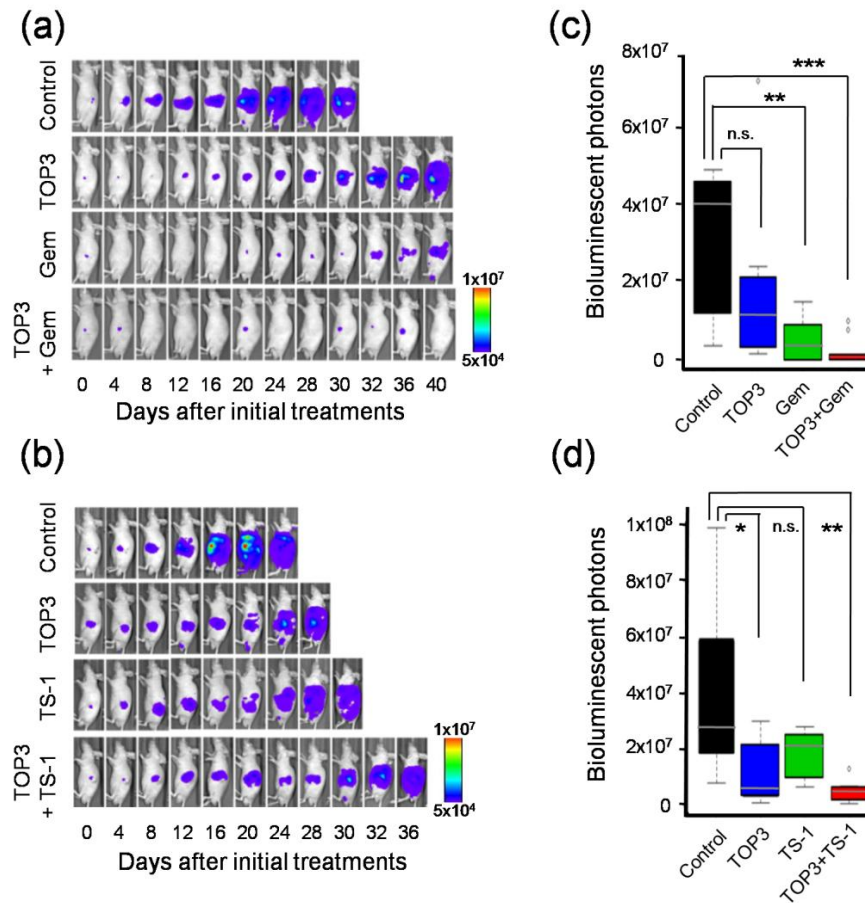
Figure 4.4: Combination therapies significantly improved outcome in a SUIT-2 orthotopic pancreatic cancer model. (**a**, **b**) Representative images of mice in each group obtained by *in vivo* imaging. (**c**, **d**) Box plots of

bioluminescent intensities of tumors in mice of gemcitabine- and TS-1-treated groups at day 20 and day 16, respectively, which were the last days that all mice in the control groups were still alive.

Table 4.4. *P*-values in comparison of bioluminescent signals of each pair group using Tukey's honest significant difference test of **Figure 4.4c, d**.

	TOP3	Gem	TOP3 + Gem
Control	0.2	0.001	0.0001
TOP3	-	0.3	0.2
Gem	-	-	1
	TOP3	TS-1	TOP3 + TS-1
Control	0.03	0.1	0.004
TOP3	-	0.9	0.9
TS-1	-.	-	0.5

During the experiments, I also examined possible side effects of the drugs on treated mice, using weight loss as an indicator. Although some mice temporarily lost weight during the experiment period, the weight of the mice varied by less than 5% of their body weight with no significant differences (**Figure 4.5**). Diarrhea was observed in TS-1 monotherapy and TS-1 combination groups, but other adverse side effects such as jaundice or change of stool colors were not observed.
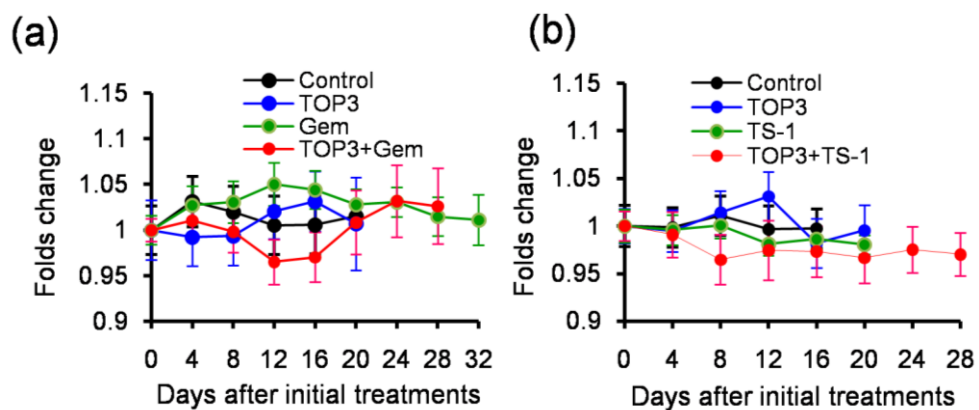
Figure 4.5: Changes in body weight of mice during treatment with (**a**) gemcitabine and (**b**) TS-1 experiments.

As an important outcome of cancer therapy, I evaluated the survival rate of the mice in each group. The results of this analysis correlated with the bioluminescence signal

development; combinations of TOP3 and gemcitabine showed the most prolonged survival rates among the treated mice. Interestingly, there was no statistically significant difference between TOP3 and TS-1 monotherapies in bioluminescence signal suppression and survival improvement (**Figure 4.4d and 4.6b**), indicating equivalent overall efficacy of the prodrug TOP3 and TS-1. Two mice in the combination group survived until day 50. SUIT-2 cells showed higher sensitivity to gemcitabine monotherapy at the selected dosage; treatment with gemcitabine resulted in remarkable inhibition of cancer cell growth and more significantly prolonged the survival of the mice than TOP3 monotherapy (**Figure 4.6a**). Combination therapy with gemcitabine and TOP3 further improved the survival. Two mice in the combination group survived for more than 100 days after initial treatment with almost complete clearance of HIF-active cell signals. The summary of significant values is indicated in **Table 4.5**.
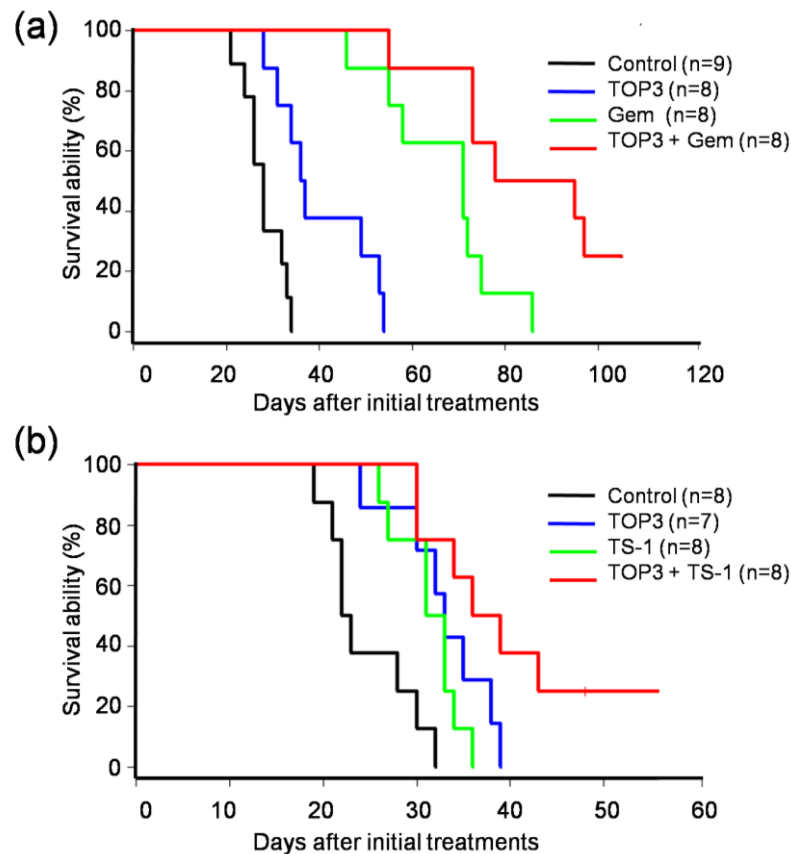
Figure 4.6: Combination therapies improved the survival of treated mice. Survival curves using Kaplan-Meier analysis in (**a**) gemcitabine- and (**b**) TS-1-treated groups.

Table 4.5. *P*-values in comparison of survival ability of each pair group using log-rank test of **Figure 4.6**.

	TOP3	Gem	TOP3 + Gem
Control	0.002	0.00003	0.00003
TOP3	-	0.0003	0.00004
Gem	-	-	0.01
	TOP3	TS-1	TOP3 + TS-1
Control	0.01	0.04	0.0001
TOP3	-	0.1	0.02
TS-1	-	-	0.003

Discussion

Traditionally, the progression of cancer cells can only be achieved by measurement of the tumor volume in subcutaneous models or by sacrifice of the animals in orthotopic models. *In vivo* imaging, therefore, by giving real-time information of the cancer cells provides overwhelming benefits over the traditional methods. Since the permeability of bioluminescence *in vivo* is much better than that of fluorescence, a luciferase reporter system offers sensitive, quantitative and real-time spatio-temporal analysis of the tumor cells. In my research, I took advantages of *in vivo* bioluminescent imaging (BLI) to monitor HIF-active cancer by HIF-dependent reporter which has been extensively studied [17, 19]. I have established SUIT-2/HRE-Luc cells expressing luciferase activity in hypoxia significant higher than in normoxia and I confirmed that the luciferase activity is highly correlated with HIF expression level (**Figure 4.2**). Consistent with previous research, I confirmed that the optical imaging method using 5HRE-luciferase reporter gene enables us to efficiently and easily visualize HIF-active hypoxia in living animals, and precisely evaluate the efficacy of anti-cancer therapies on tumor hypoxia.

For orthotopic model, I used SUIT-2 cell line which is derived from a metastatic liver tumor of human pancreatic carcinoma which carries KRas mutation and c-Met positive. Orthotopic transplantation of SUIT-2 has been reported as a clinically relevant model showing an aggressive and malignant phenotype with liver metastasis, peritoneal dissemination and ascites [20, 21]. My transplantation model in this research successfully characterized all the above phenomena of severe pancreatic cancer. All the mice in the control groups died in less than 40 days after transplantation with accumulation of peritoneal dissemination and fulminant ascites (**Figure 4.6**). The fact that HIF-active cancer cells can be well-visualized in this model consolidates previous observation in clinical samples which indicated that pancreatic cancer is extremely hypoxic compared with the surrounding normal tissue or other cancer tumor types [22, 23].

References

1. Bardeesy, N. and R.A. DePinho, *Pancreatic cancer biology and genetics.* Nat Rev Cancer, 2002. **2**(12): p. 897-909.

2. Erickson, L.A., et al., *Targeting the hypoxia pathway to treat pancreatic cancer.* Drug Des Devel Ther, 2015. **9**: p. 2029-31.

3. Sheikh, R., et al., *Challenges of drug resistance in the management of pancreatic cancer.* Expert Rev Anticancer Ther, 2010. **10**(10): p. 1647-61.

4. Zeman, E.M., et al., *SR-4233: a new bioreductive agent with high selective toxicity for hypoxic mammalian cells.* Int J Radiat Oncol Biol Phys, 1986. **12**(7): p. 1239-42.

5. Colucci, M.A., C.J. Moody, and G.D. Couch, *Natural and synthetic quinones and their reduction by the quinone reductase enzyme NQO1: from synthetic organic chemistry to compounds with anticancer potential.* Organic & Biomolecular Chemistry, 2008. **6**(4): p. 637-656.

6. Hu, J., et al., *Targeting the multiple myeloma hypoxic niche with TH-302, a hypoxia-activated prodrug.* Blood, 2010. **116**(9): p. 1524-7.

7. Guise, C.P., et al., *Identification of human reductases that activate the dinitrobenzamide mustard prodrug PR-104A: A role for NADPH : cytochrome P450 oxidoreductase under hypoxia.* Biochemical Pharmacology, 2007. **74**(6): p. 810-820.

8. Raleigh, S.M., et al., *Involvement of human cytochromes P450 (CYP) in the reductive metabolism of AQ4N, a hypoxia activated anthraquinone di-N-oxide prodrug.* Int J Radiat Oncol Biol Phys, 1998. **42**(4): p. 763-7.

9. Danson, S.J., et al., *Phase I pharmacokinetic and pharmacodynamic study of the bioreductive drug RH1.* Ann Oncol, 2011. **22**(7): p. 1653-60.

10. Papadopoulou, M.V. and W.D. Bloomer, *NLCQ-1 (NSC 709257): exploiting hypoxia with a weak DNA-intercalating bioreductive drug.* Clin Cancer Res, 2003. **9**(15): p. 5714-20.

11. Rischin, D., et al., *Tirapazamine, cisplatin, and radiation versus cisplatin and radiation for advanced squamous cell carcinoma of the head and neck (TROG 02.02, HeadSTART): a phase III trial of the Trans-Tasman Radiation Oncology Group.* J Clin Oncol, 2010. **28**(18): p. 2989-95.

12. Williamson, S.K., et al., *Phase III trial of paclitaxel plus carboplatin with or without tirapazamine in advanced non-small-cell lung cancer: Southwest Oncology Group Trial S0003.* J Clin Oncol, 2005. **23**(36): p. 9097-104.

13. DiSilvestro, P.A., et al., *Phase III randomized trial of weekly cisplatin and irradiation versus cisplatin and tirapazamine and irradiation in stages IB2, IIA,*

IIB, IIIB, and IVA cervical carcinoma limited to the pelvis: a Gynecologic Oncology Group study. J Clin Oncol, 2014. **32**(5): p. 458-64.

14. Konopleva, M., et al., *Phase I/II study of the hypoxia-activated prodrug PR104 in refractory/relapsed acute myeloid leukemia and acute lymphoblastic leukemia.* Haematologica, 2015. **100**(7): p. 927-34.

15. Harada, H., et al., *Significance of HIF-1-active cells in angiogenesis and radioresistance.* Oncogene, 2007. **26**(54): p. 7508-16.

16. Harada, H., M. Hiraoka, and S. Kizaka-Kondoh, *Antitumor effect of TAT-oxygen-dependent degradation-caspase-3 fusion protein specifically stabilized and activated in hypoxic tumor cells.* Cancer Res, 2002. **62**(7): p. 2013-8.

17. Kizaka-Kondoh, S., et al., *Selective killing of hypoxia-inducible factor-1-active cells improves survival in a mouse model of invasive and metastatic pancreatic cancer.* Clin Cancer Res, 2009. **15**(10): p. 3433-41.

18. Semenza, G.L., *Hypoxia-inducible factor 1: oxygen homeostasis and disease pathophysiology.* Trends Mol Med, 2001. **7**(8): p. 345-50.

19. Kadonosono, T., et al., *Detection of the onset of ischemia and carcinogenesis by hypoxia-inducible transcription factor-based in vivo bioluminescence imaging.* PLoS One, 2011. **6**(11): p. e26640.

20. Tomioka, D., et al., *Inhibition of growth, invasion, and metastasis of human pancreatic carcinoma cells by NK4 in an orthotopic mouse model.* Cancer Res, 2001. **61**(20): p. 7518-24.

21. Shono, M., et al., *Stepwise progression of centrosome defects associated with local tumor growth and metastatic process of human pancreatic carcinoma cells transplanted orthotopically into nude mice.* Lab Invest, 2001. **81**(7): p. 945-52.

22. Koong, A.C., et al., *Pancreatic tumors show high levels of hypoxia.* Int J Radiat Oncol Biol Phys, 2000. **48**(4): p. 919-22.

23. Brown, J.M. and W.R. Wilson, *Exploiting tumour hypoxia in cancer treatment.* Nat Rev Cancer, 2004. **4**(6): p. 437-47.

Chapter 5

Concluding remarks and future perspectives

Targeting solid tumors has become an imperative goal to overcome treatment resistance and prolong survival rates of several refractory cancers. Among them, therapeutic treatments for hypoxic pancreatic cancers are urgently needed to overcome the limitation of current regimens. In our lab, we have developed a fusion protein TOP3 which specifically targets HIF-active cancers. TOP3 has proven its anti-tumor effects on various cancer cell lines and mice models. However, the efficacy of TOP3 in combination with therapeutic drugs has not been evaluated. In this thesis, I evaluated the efficacy of HIF-targeting prodrug TOP3 in comparison with the standard drugs gemcitabine and TS-1 for pancreatic cancer treatment in order to get further insights into the treatment efficacy of hypoxic cancer using these combination therapies. For this purpose, I first confirmed that pancreatic cancers are resistant to these chemotherapeutic drugs when they were exposed to conditions with reduced oxygen levels (**Chapter 2**). On the other hand, TOP3 efficiently induced cell death under hypoxic and starved conditions, suggesting promising treatment by TOP3 combined with gemcitabine and TS-1 (**Chapter 3**). When TOP3 was combined with gemcitabine or TS-1 to treat mice bearing orthotopic tumors, the treatments successfully suppressed the progression of tumors and prolonged the survival of the mice, resulting in the most outstanding outcomes among the treatments (**Chapter 4**).

Chapter 2 describes an evaluation about response of normoxic and hypoxic pancreatic cancer cells to the drugs gemcitabine and TS-1. It has been reported that pancreatic cancers contain both normoxic and hypoxic cancer cells which are often resistant to chemotherapeutic treatments. When being exposed to hypoxic (0.1% O_2) and severe hypoxic (0.1% O_2) conditions, human pancreatic cancer cell SUIT-2 exhibited resistance to the drugs to different degrees, which was confirmed by both WST-1 and Calcein AM proliferation assays. Thus, treatment of pancreatic cancers by only chermotherapeutics drugs are insufficient to completely eradicate pancreatic cancers, suggesting promising outcomes by TOP3 *in vitro* and *in vivo* in combination with these chemotherapeutic drugs.

Chapter 3 describes the treatment efficacy of TOP3 on cancer cells under tumor hypoxia-mimic conditions by culturing pancreatic cancer cells with starved medium and reduced oxygen levels. The pancreatic cander cells were treated with TOP3 alone or in combination with gemcitabine and TS-1 under hypoxia-mimic conditions (1% O_2, 500 mg/L glucose, 0.2% FBS) and severe hypoxia-mimic conditions (0.1% O_2, 100 mg/L glucose, 0.1% FBS). Flow cytometry analysis of sub-G1 fraction in the treated pancreatic cancer cell genomes using propidium iodide confirmed cell death induction by TOP3 under

hypoxic and severe hypoxic conditions but not normoxic conditions. These results together with the results of Chapter 2 demonstrate that TOP3 targets distinct cell populations from gemcitabine and TS-1, and suggest that combination treatment of pancreatic cancers by TOP3 in combination with these chemotherapeutic drugs may improve treatment outcomes of pancreatic cancer patients.

Chapter 4 describes *in vivo* evaluation of efficacy of TOP3 using orthotopic pancreatic cancer model mice. Pancreatic cancer cells SUIT-2 was first stably transfected with a reporter vector encoding a firefly luciferase protein under the control of a HIF-dependent promoter. Therefore, the cells generate bioluminescent signals correlated with the expression levels of HIF proteins and thus allow us to noninvasively monitor HIF activity in tumors in real-time. The tumor-bearing mice were treated by monotherapy of TOP3, gemcitabine and TS-1, or by TOP3 combined with gemcitabine or TS-1. The treatment of the mice with TOP3, gemcitabine or TS-1 suppressed HIF activity in the cancers, and the combination treatments further reduced intratumoral HIF-activity while inducing no apparent side effects. Moreover, survival of the treated mice was reversely correlated with the intratumal HIF-activity, suggesting the potentials of treatment by TOP3 in combination with these chemotherapeutic drugs for pancreatic cancer patients.

The final goal of this study is further evaluation of the effects of TOP3 on other solid tumors before proceeding to clinical trials, and ultimately making TOP3 applicable for HIF-active cancers. To achieve the goal, in our lab, three concomitant projects have been proceeding. The first one is improvement of TOP3 purity by modulating TOP3 structure and purification method. I have employed several approaches such as purification of His-tagged TOP3, periplasmic production of TOP3 or expression in mammalian cells. However, these approaches did not improve the purity. Nevertheless, after optimizing several parameters for cultivation including IPTG concentrations, temperature and shaking speeds, etc., TOP3 became one of the major products in E. *coli* and was succeeded to purify using Fast Protein Liquid Chromatography (FPLC) of the E. *coli* lysate supernatant after ammonium sulfate percipitation, achieving almost 100% purity. In addition, the protocol for a large-scale production of high purity TOP3 is under development in cooperation with a company to produce TOP3 in good manufacturing practice (GMP) level for pre-clinical trials. Secondly, other suitable models will be established to further explore the effects of TOP3 in other HIF-active hypoxic cancers. One of our best candidates for the models is employment of 786-O renal cell carcinoma since this cell line has mutation in *VHL* gene and expresses no VHL, leading to the stable expression of HIF even under

normoxic conditions. Thus, I expect that TOP3 which is under the same VHL oxygen-dependent regulation as HIFα proteins may provide the effects to all stressed renal cancer cells regardless of their oxygen status. Furthermore, I also consider evaluating TOP3 efficacy in other reported hypoxic cancers such as lung, prostate and cervical cancers. Finally, further analyses of TOP3 properties such as the biodistribution, pharmacokinetic as well as pharmacodynamics of the protein after administration are being conducted. By labelling TOP3 with radioisotopes such as Iodine-125 and employing positron emission tomography/single photon emission computed tomography, the distribution, accumulation and retention of TOP3 in specific tissues can be traced and evaluated although we have to carefully distinguish the signals from intact TOP3 from free Iodine-125 released from degraded TOP3 in off-target tissues. By this technique, it is also possible to evaluate possible side effects of TOP3 due to unfavorable accumulation in non-cancerous tissue cells. Furthermore, isotope-labelled TOP3 can be used as a companion diagnostic tool for TOP3: for identifying patients who may respond to TOP3.

Overall, I hope that the potentials of TOP3 will be fully evaluated in subsequent studies, and eventually the prodrug TOP3 will be available to treat HIF-active cancer cells in several solid tumors. Therefore, TOP3 can contribute to the treatment of these refractory cancers and bring benefits to cancer patients.

Achievements

I. Poster presentations:

1. <u>Thi Hong Ngoc Hoang</u>, Ryutaro Ishikawa, Akane Kanamori, Takahiro Kuchimaru, Tetsuya Kadonosono, Shinae Kizaka-Kondoh. "**Evaluation of POP33, a protein drug targeting HIF-active cancers, in an orthotopic pancreatic cancer model**", *The 17th Annual Meeting of the Japanese Association for Molecular Target Therapy for Cancer*, Kyoto, Japan, **June 2013**.

2. <u>Thi Hong Ngoc Hoang</u>, Nguyen The Kha, Takahiro Kuchimaru, Tetsuya Kadonosono, Shinae Kizaka-Kondoh. "**Establishment of LM8 osteosarcoma sublines to identify responsible genes for lung metastasis**", *The 37th Annual Meeting of the Molecular Biology Society of Japan*, Yokohama, Japan, **November 2014**.

3. <u>Thi Hong Ngoc Hoang</u>, Tetsuya Kadonosono, Takahiro Kuchimaru, Shinae-Kizaka Kondoh. "**Enhanced antitumor effects of TOP3 and TS-1 combination therapy for pancreatic cancer treatment**", *The 12th Annual meeting of Japanese Association for Cancer and Hypoxia Research*, Saga, Japan, **November 2014**.

4. <u>Thi Hong Ngoc Hoang</u>. Tetsuya Kadonosono, Takahiro Kuchimaru, Shinae-Kizaka Kondoh."**Enhanced antitumor effects of TOP3 and gemcitabine combination therapy for pancreatic cancer treatment**", *The 13th Annual meeting of Japanese Association for Cancer and Hypoxia Research,* Shizuoka, Japan, **June 2015**.

5. <u>Thi Hong Ngoc Hoang</u>. Tetsuya Kadonosono, Takahiro Kuchimaru, Shinae-Kizaka Kondoh. "**Enhanced antitumor effects of TOP3 and chemotherapeutic drugs in combination therapy for pancreatic cancer treatment**", *The 74th Annual Meeting of the Japanese Cancer Association*, Nagoya, Japan, **October 2015**.

II. Published papers

Hoang, N.T., Kadonosono T, Kuchimaru T, Kizaka-Kondoh S, *Hypoxia-inducible factor-targeting prodrug TOP3 combined with gemcitabine or TS-1 improves pancreatic cancer survival in an orthotopic model.* Cancer Sci, 2016. **107**(8): p. 1151-8. doi: 10.1111/cas.12982

Acknowledgements